



U.S. Department of
Transportation

**Federal Railroad
Administration**

Load Environment of Rail Joint Bars – Phase III Assessment of the Effects of Installation and Maintenance Practices

Office of Research
and Development
Washington, DC 20590



NOTICE

This document is disseminated under the sponsorship of the Department of Transportation in the interest of information exchange. The United States Government assumes no liability for its contents or use thereof. Any opinions, findings and conclusions, or recommendations expressed in this material do not necessarily reflect the views or policies of the United States Government, nor does mention of trade names, commercial products, or organizations imply endorsement by the United States Government. The United States Government assumes no liability for the content or use of the material contained in this document.

NOTICE

The United States Government does not endorse products or manufacturers. Trade or manufacturers' names appear herein solely because they are considered essential to the objective of this report.

REPORT DOCUMENTATION PAGE			<i>Form Approved</i> <i>OMB No. 0704-0188</i>	
Public reporting burden for this collection of information is estimated to average 1 hour per response, including the time for reviewing instructions, searching existing data sources, gathering and maintaining the data needed, and completing and reviewing the collection of information. Send comments regarding this burden estimate or any other aspect of this collection of information, including suggestions for reducing this burden, to Washington Headquarters Services, Directorate for Information Operations and Reports, 1215 Jefferson Davis Highway, Suite 1204, Arlington, VA 22202-4302, and to the Office of Management and Budget, Paperwork Reduction Project (0704-0188), Washington, DC 20503.				
1. AGENCY USE ONLY (Leave blank)		2. REPORT DATE August 2015		1. AGENCY USE ONLY (Leave blank) August 2014
4. TITLE AND SUBTITLE Load Environment of Rail Joint Bars – Phase III Assessment of the Effects of Installation and Maintenance Practices			5. FUNDING NUMBERS Contract DTFR53-11-D-00008 Task Order 306	
6. AUTHOR(S) Jay Baillargeon, ⁽¹⁾ David Jeong, ⁽²⁾ Muhammad Akhtar, ⁽¹⁾ Curt Mademann, ⁽¹⁾ and David Davis ⁽¹⁾				
7. PERFORMING ORGANIZATION NAME(S) AND ADDRESS(ES) ⁽¹⁾ Transportation Technology Center, Inc. A Subsidiary of the Association of American Railroads PO Box 11130 Pueblo, CO 81001 ⁽²⁾ U.S. Department of Transportation Volpe National Transportation Systems Center 55 Broadway Cambridge, MA 02142			8. PERFORMING ORGANIZATION REPORT NUMBER	
9. SPONSORING/MONITORING AGENCY NAME(S) AND ADDRESS(ES) U.S. Department of Transportation Federal Railroad Administration Office of Research, Development, and Technology Washington, DC 20590			10. SPONSORING/MONITORING AGENCY REPORT NUMBER DOT/FRA/ORD-15/26	
11. SUPPLEMENTARY NOTES COTR: Luis Maal				
12a. DISTRIBUTION/AVAILABILITY STATEMENT This document is available to the public through the FRA Web site at http://www.fra.dot.gov .			12b. DISTRIBUTION CODE	
13. ABSTRACT (Maximum 200 words) A series of tests, aimed at assessing the structural integrity of joint bars under differing service conditions, were conducted to address concerns regarding joint bar failures in the revenue service environment. Data collected through the course of this study revealed that bending stress invoked by normal track surfacing operations is not a likely cause for cracks that initiate at the top center of joint bars. Instead, cracking at this location is probably the result of fatigue at the top center of the joint bar due to rail-joint contact. Surface hardening at the area of rail-joint contact was largely ineffective, resulting in metal flow developing adjacent to the easement at the top of the joint bar. Additional data gathered in this study suggests little correlation between the surface hardness of the joint bar and the depth of metal flow. Bending stresses and wheel/rail forces were also measured on joint bars used in rail end gaps and rail height mismatches, which revealed minimal effects on overall joint bar performance for the installation conditions and range of speeds evaluated.				
14. SUBJECT TERMS Rail joint bars, joint bar failures, finite element analysis			15. NUMBER OF PAGES 59	
			16. PRICE CODE	
17. SECURITY CLASSIFICATION OF REPORT Unclassified	18. SECURITY CLASSIFICATION OF THIS PAGE Unclassified	17. SECURITY CLASSIFICATION OF REPORT Unclassified	18. SECURITY CLASSIFICATION OF THIS PAGE Unclassified	

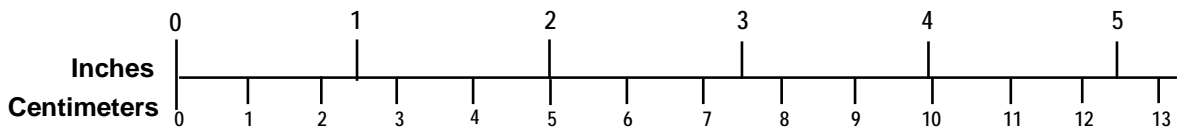
METRIC/ENGLISH CONVERSION FACTORS

ENGLISH TO METRIC

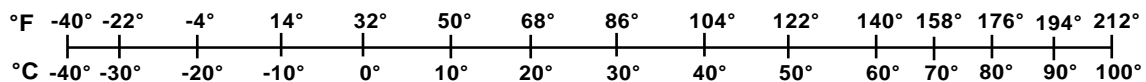
METRIC TO ENGLISH

<p>LENGTH (APPROXIMATE)</p> <p>1 inch (in) = 2.5 centimeters (cm)</p> <p>1 foot (ft) = 30 centimeters (cm)</p> <p>1 yard (yd) = 0.9 meter (m)</p> <p>1 mile (mi) = 1.6 kilometers (km)</p>	<p>LENGTH (APPROXIMATE)</p> <p>1 millimeter (mm) = 0.04 inch (in)</p> <p>1 centimeter (cm) = 0.4 inch (in)</p> <p>1 meter (m) = 3.3 feet (ft)</p> <p>1 meter (m) = 1.1 yards (yd)</p> <p>1 kilometer (km) = 0.6 mile (mi)</p>
<p>AREA (APPROXIMATE)</p> <p>1 square inch (sq in, in²) = 6.5 square centimeters (cm²)</p> <p>1 square foot (sq ft, ft²) = 0.09 square meter (m²)</p> <p>1 square yard (sq yd, yd²) = 0.8 square meter (m²)</p> <p>1 square mile (sq mi, mi²) = 2.6 square kilometers (km²)</p> <p>1 acre = 0.4 hectare (he) = 4,000 square meters (m²)</p>	<p>AREA (APPROXIMATE)</p> <p>1 square centimeter (cm²) = 0.16 square inch (sq in, in²)</p> <p>1 square meter (m²) = 1.2 square yards (sq yd, yd²)</p> <p>1 square kilometer (km²) = 0.4 square mile (sq mi, mi²)</p> <p>10,000 square meters (m²) = 1 hectare (ha) = 2.5 acres</p>
<p>MASS - WEIGHT (APPROXIMATE)</p> <p>1 ounce (oz) = 28 grams (gm)</p> <p>1 pound (lb) = 0.45 kilogram (kg)</p> <p>1 short ton = 2,000 pounds (lb) = 0.9 tonne (t)</p>	<p>MASS - WEIGHT (APPROXIMATE)</p> <p>1 gram (gm) = 0.036 ounce (oz)</p> <p>1 kilogram (kg) = 2.2 pounds (lb)</p> <p>1 tonne (t) = 1,000 kilograms (kg) = 1.1 short tons</p>
<p>VOLUME (APPROXIMATE)</p> <p>1 teaspoon (tsp) = 5 milliliters (ml)</p> <p>1 tablespoon (tbsp) = 15 milliliters (ml)</p> <p>1 fluid ounce (fl oz) = 30 milliliters (ml)</p> <p>1 cup (c) = 0.24 liter (l)</p> <p>1 pint (pt) = 0.47 liter (l)</p> <p>1 quart (qt) = 0.96 liter (l)</p> <p>1 gallon (gal) = 3.8 liters (l)</p> <p>1 cubic foot (cu ft, ft³) = 0.03 cubic meter (m³)</p> <p>1 cubic yard (cu yd, yd³) = 0.76 cubic meter (m³)</p>	<p>VOLUME (APPROXIMATE)</p> <p>1 milliliter (ml) = 0.03 fluid ounce (fl oz)</p> <p>1 liter (l) = 2.1 pints (pt)</p> <p>1 liter (l) = 1.06 quarts (qt)</p> <p>1 liter (l) = 0.26 gallon (gal)</p> <p>1 cubic meter (m³) = 36 cubic feet (cu ft, ft³)</p> <p>1 cubic meter (m³) = 1.3 cubic yards (cu yd, yd³)</p>
<p>TEMPERATURE (EXACT)</p> <p>$[(x-32)(5/9)]\text{ }^\circ\text{F} = y\text{ }^\circ\text{C}$</p>	<p>TEMPERATURE (EXACT)</p> <p>$[(9/5)y + 32]\text{ }^\circ\text{C} = x\text{ }^\circ\text{F}$</p>

QUICK INCH - CENTIMETER LENGTH CONVERSION



QUICK FAHRENHEIT - CELSIUS TEMPERATURE CONVERSION



For more exact and or other conversion factors, see NIST Miscellaneous Publication 286, Units of Weights and Measures. Price \$2.50 SD Catalog No. C13 10286

Updated 6/17/98

Contents

Executive Summary	1
1. Introduction	3
1.1 Background	3
1.2 Objectives	4
1.3 Overall Approach	4
1.4 Scope	5
1.5 Organization of the Report	5
2. Common Joint Bar Failure Modes	6
3. Effects of Track Surfacing on Joint Bar Stresses	11
3.1 Test Setup	11
3.2 Results and Discussion	13
4. Effects of Bolt Torque Loss on Joint Bars	17
4.1 Induction Hardening of Joint Bars	17
4.2 Test Setup	18
4.3 Results and Discussion	19
5. Effects of Railhead Gaps and Mismatches on Joint Bars	22
5.1 Test Setup	22
5.2 Results and Discussion	24
6. Metal Flow versus Crack Propagation in Joint Bars	29
6.1 Test Setup	29
6.2 Results and Discussion	30
7. Finite Element Analysis of Bolted Rail Joint	32
8. Industry Design Developments	55
9. Conclusions	58
10. References	59
Abbreviations and Acronyms	60

Illustrations

Figure 1. Top Center Crack	7
Figure 2. Joint Bar Bolt Hole Crack	7
Figure 3. Bottom Center Crack.....	8
Figure 4. Bottom Edge Crack	8
Figure 5. Quarter Crack and Quarter Break.....	9
Figure 6. Distribution of Vertical Deflections for Intact and Defective Rail Joints.....	9
Figure 7. Installation of the Joint Bars in the Test Zone at FAST	11
Figure 8. Location of the Artificial Notches (left), One of the Artificial Notches at the Top of a Test Joint Bar (right).....	12
Figure 9. Placement of the Loaded Freight Car in the Test Zone.....	12
Figure 10. Location of Bending Circuits along the Central Axis	13
Figure 11. Tamper Used to Complete Surfacing Operations at FAST for this Study	13
Figure 12. Plot of the Pre-Tamping TOR Elevations for the Test Zone, for both Loaded and Unloaded Scenarios	14
Figure 13. Plot of the Post-Tamping TOR Elevations for the Test Zone, for both Loaded and Unloaded Scenarios	14
Figure 14. Stripcharts Presenting the Bending Stresses for Two of the Four Joint Bars.....	15
Figure 15. Locations of the Induction Hardened Areas on the Joint Bars.....	17
Figure 16. Diagram Noting the Location of Longitudinal Profile Measurements.....	18
Figure 17. Longitudinal Profile Measurement Locations at the Top of a Test Joint Bar	18
Figure 18. Installation of Standard and Post-Hardened Joint Bars at FAST	19
Figure 19. Pre- and Post-Test Longitudinal Profiles for an Untreated (left) and a Post-Hardened (right) Joint Bar.....	20
Figure 20. Post-Test Metal Flow for an Untreated (left) and a Post-Hardened (right) Joint Bar	20
Figure 21. Fatigue Cracking in an Untreated (left) and a Post-Hardened (right) Joint Bar.....	21
Figure 22. Installation of Instrumented Joints Bars at FAST	23
Figure 23. Plan View of an Example Railhead Mismatch Test Setup (1/2 in).....	23
Figure 24. Plots of the 95 th Percentile for IWS Vertical Wheel Force Data (Rail Gaps)	24
Figure 25. Time History for IWS Vertical Wheel Force Data (1-in Gap, 45 mph).....	25
Figure 26. Plots of the 95 th Percentile for IWS Vertical Wheel Force Data (Railhead Mismatch)	26
Figure 27. Time History for IWS Vertical Wheel Force Data (1/4-in Mismatch, 10 mph)	27

Figure 28. Box Plots of the Bending Stresses under the IWS for Each Circuit (Rail Gap).....	28
Figure 29. Box Plots of the Bending Stresses under the IWS for Each Circuit (Railhead Mismatch)	28
Figure 30. Area of Interest/Stress Concentration Location	29
Figure 31. Plot of the Height Loss Due to Metal Flow against Surface Hardness	31
Figure 32. Finite Element Model Setup for Supported and Suspended Joints	33
Figure 33. Recommended Head Easement for Head-Free Joint Bars [6].....	35
Figure 34. Joint Bar Reactions under Positive Bending	37
Figure 35. Potential Locations for Contact between Rail and Joint Bar.....	41
Figure 36. Example Prototype Joint Bar Design	47
Figure 37. Calculated Contact between Rail and Joint Bar by Design.....	48

Tables

Table 1. Subset of Joint Bar Samples	30
Table 2. Summary of Section Properties for 136 RE Rail and 132 RE Joint Bars	32
Table 3. Assumptions in FEAs of Supported and Suspended Rail Joints	34
Table 4. Assumed Bolt Patterns	34
Table 5. FEA-calculated Deflections under 35.75-kip Wheel Load.....	36
Table 6. Vertical Deflection along Length of Rail	37
Table 7. Contact Force Normal to Element Faces on Joint Bar (Supported Joint).....	39
Table 8. Contact Force Normal to Element Faces on Joint Bar (Suspended Joint).....	40
Table 9. Contours of Contact Pressure in Supported Joint under 35.75-kip Wheel Load	42
Table 10. Contours of Contact Pressure in Suspended Joint under 35.75-kip Wheel Load	43
Table 11. Bolt Tension in Supported Joint Before and After 35.75-kip Wheel Load	45
Table 12. Bolt Tension in Suspended Joint Before and After 35.75-kip Wheel Load	46

Executive Summary

This report is the third in a three-part series on investigations conducted by the Transportation Technology Center, Inc. (TTCI) into the effect of load environment on joint bar structural integrity [1,2]. The joint bar is the only track component that has not changed for many decades—the cross-section has increased to match increasing rail sizes, but the basic design has remained the same. Unlike other track components, where component-caused accidents have gradually been reduced due to design improvements, the number of joint bar related accidents has remained the same.

Under the Federal Railroad Administration (FRA) Track research program, Transportation Technology Center, Inc. (TTCI) is investigating various options to reduce joint bar failures. In these investigations, several tests were performed that examined the influence of joint bar designs, joint bar materials, track design, and track maintenance on joint bar structural integrity. These tests were conducted at the United States Department of Transportation's Transportation Technology Center (TTC) near Pueblo, Colorado and the work described in these reports was funded by the Federal Railroad Administration's (FRA) Office of Research, Development, and Technology (ORD).

TTCI, in collaboration with ENSCO, Inc., conducted field surveys of rail joints in revenue service track. Automated and visual inspections identified defective joint bars and detailed information and measurements were collected at various joint locations, including randomly selected intact (i.e., non-defective) joints to establish a control group to help identify factors that might affect joint bar failure. The most common joint bar failure modes observed in these field surveys are described in this report.

Tests were conducted at TTC's Facility for Accelerated Service Testing (FAST) to measure strains in instrumented rail joints during track maintenance activities. Test data revealed that the lifting of the joint bars during track surfacing operations is probably not the cause of joint bar cracks initiating at the top of the bars. Tensile bending stresses at the top of the joint bars were found to be lower than those observed under normal train operations. The measured bending stresses at the top of the joint bars were largely in compression and relatively low while the tamper raised the joints to 1 inch or more.

Tests were also conducted at FAST to monitor dynamic loads at instrumented rail joints and examine the effects of rail end and rail height mismatches under heavy axle load (HAL) conditions. The effects of varying the rail end gap from 0 to 1 inch in were notably small over the range of test speeds between 10 and 45 miles per hour (mph) with regard to measured wheel/rail forces using instrumented wheel sets (IWS) with a limited capacity for capturing higher frequency impact forces. Similarly, the effects of varying rail height mismatch from 0 to 0.25 inch were relatively small with regard to the tensile bending stresses measured at the top and bottom of the joint bars.

Crack initiation at the top center of the joint bar is likely the result of notching due to continued cyclical contact with the end of the railhead under passing loads. Surface hardening of joint bars, which is intended to improve the resistance to notching in areas of contact between the railhead and the top of the joint bar, was found to be ineffective. A comparison of hardened and unhardened joint bars HAL operations revealed that both resulted in metal flow at the top of

them. A thorough inspection of 100 sample joint bars from revenue service and rail joints at TTC revealed little correlation between the surface hardness of the joint bars and the depth of metal flow at the top center of the bars. Surface hardening might provide some benefit in reducing the amount of metal flow in terms of reducing the loss of bolt torque. However, even with surface hardening, the contact conditions are severe enough to cause plastic deformation. These findings suggest that a review of the joint bar easement design may be beneficial.

Finite element analyses (FEAs) were conducted by the Volpe National Transportation Systems Center (Volpe) to simulate the structural response of bolted rail joints under varying loading and support conditions. These FEAs were also used to estimate contact stresses between the rail and the joint bar. The results of these analyses showed that vertical deflection depends strongly on support conditions in the vicinity of the joint. These results are consistent with observations and measurements collected during the field surveys and with results from previous tests described in the Phase I report [1]. FEA results also show that the locations of contact and the relative magnitude of the contact pressure between the rail and the joint bar depend on the number of bolts as well as support conditions. In addition, the FEA results indicate that the relative magnitude of contact forces at the top of the joint bar is reduced when an easement is present.

1. Introduction

This report is the third in a three-part series that studies the effect of load environment on rail joint bar structural integrity. In the Phase I report, Transportation Technology Center, Inc. (TTCI) measured bending stresses, thermal stresses, and residual stresses in joint bars under a variety of loading and track conditions [1]. Phase II continued to study stresses in joint bars but with a particular focus on the cyclic behavior which contributes to metal fatigue [2]. The Phase II report also described measurements of residual stresses, and how they affect the fatigue and yield strength properties of the joint bar material.

This report describes studies which provided insights into why and how joint bars develop fatigue cracks by: (1) examining the causes and locations of crack initiation, and (2) quantifying the effects of various track parameters that may cause overstressing. In this report, the potential causes for overstress that were examined were: (a) lifting of the joint during track maintenance (i.e. track surfacing), (b) loss of bolt torque under repeated wheel passages, and (c) dynamic load amplification at rail joints due to rail end gaps and head height mismatches.

Ultimately the results of this series of reports will help develop guidelines for best practices and potential methods that reduce the occurrence of joint bar failures in revenue service.

1.1 Background

The bolted rail joint bar that is used today in continuous welded rail (CWR) territory was designed in the early 1900s to provide vertical and horizontal rail alignment while allowing for longitudinal movement to offset rail expansion and contraction due to temperature changes. In CWR territory, joint bars must also resist longitudinal loads due to wheel loads from passing trains.

In terms of mechanical performance, rail joints are thought to be a weak link because the section properties (i.e., cross-sectional area and area moment of inertia) are typically less than those for the rail itself. Joint bar failures have become a major safety concern for the freight railway industry due to several factors, including the following:

- Increasing wheel loads. The average wheel loads have increased over the past 50 years. New rail sections have been designed to accommodate increased wheel loads. The joint bar cross section has also increased to match increasing rail sizes, but the basic design has remained the same.
- Increased traffic density. Over the past 20 years, average tonnage rates have doubled which, in turn, has increased the rate of loading cycles on any given rail joint in revenue service.
- Interchangeability of joint bars on various mainline rails. This practice facilitates the perpetual use of joint bars until they fail.
- High-profile accidents related to joint bar failures. A review of Federal Railroad Administration (FRA) accident data from FRA's Rail Accident/Incident Reporting System (RAIRS) indicates that, since 2000, about 20 joint-related accidents occur each year on average. Although such accidents are relatively rare events compared to other

track-caused accidents, recent train derailments and collisions have occurred that resulted in severe consequences because the trains involved were carrying passengers or hazardous materials.

1.2 Objectives

These primary objectives address key areas of concern regarding joint bar failures in CWR territory:

- Summarize the most common joint bar failures found in mainline revenue service environment
- Investigate the potential effects regular maintenance practices (e.g., track surfacing) have on the integrity of joint bars in CWR
- Determine the effects of bolt torque loss on the performance of joint bars under heavy axle load (HAL) traffic
- Investigate the effects of railhead gaps and mismatches on vertical wheel forces and the associated bending stresses in joint bars
- Evaluate the relationship between metal flow and crack propagation in joint bars
- Estimate the contact stresses between the parent rail and the joint bar through finite element analysis (FEA)

In addition, the secondary objectives of this study, stemming from the results of the primary objectives, were the following:

- Recommend guidelines for improved joint bar inspection and maintenance
- Recommend measures to reduce performance concerns about joint bars currently utilized in CWR mainline track

1.3 Overall Approach

To meet the objectives of this study, the following tasks were completed:

- Collaborated with ENSCO, Inc. to conduct field surveys of joint bars in revenue service and develop a database to document observations and measurements at failed and intact joint locations
- Instrumented commonly used joint bars and installed them at TTCI's Facility for Accelerated Service Testing (FAST) in order to measure the bending stresses resulting from normal track surfacing operations
- Instrumented commonly used joint bars and installed them at FAST, then combined them with controlled test runs of instrumented wheelsets (IWS), in order to measure the bending stresses and vertical dynamic forces exerted on joint bars while in the presence of gaps and railhead mismatches
- Installed standard and post-hardened joint bars at FAST and measured the material flow accumulated following 55 million gross tons (MGT) of HAL traffic

- Collaborated with the Volpe National Transportation Systems Center to conduct FEA on rail joints under various loading and support conditions

1.4 Scope

The scope of the project includes all North American freight railroad operations on mainline tracks, which constitute the majority of the risk in terms of accident severity and impact on public safety. These lines also have the most severe loading environments.

The majority of the laboratory and field test work has been conducted using “modern” joint bar designs and rail sections. This includes 6-in base rails and short-toe joint bars.

1.5 Organization of the Report

Section 2 of this report summarizes field surveys conducted by TTCI and ENSCO to collect data on joint bar defects and failures on two Class 1 railroads. This section also describes the most common joint bar defects and failure modes discovered during these surveys.

The subsequent sections describe various tests which quantify the effects of various track parameters that may cause overstressing of the joint bar. Section 3 describes tests which analyze the effects of track surfacing on joint bar stresses. In Section 4, the effect of bolt torque loss under heavy axle loads is examined. Section 5 describes an investigation into the effects of railhead gap and mismatch on joint bar integrity by measuring dynamic wheel loads at rail joints. Section 6 determines if a correlation exists between the amount of metal flow and the propagation of cracking in joint bars. If such a correlation exists, this knowledge could be used to develop a fit-for-service criterion for reusing joint bars in track.

Section 7 presents results from FEAs of bolted rail joints under various loading and support conditions. These analyses serve to interpret the information and measurements collected during the field surveys on revenue service track and explain results from the various tests conducted by TTCI to study the load environment on rail joint bars.

Finally, Section 8 summarizes the conclusions from Phase III of the three-part series of investigations.

2. Common Joint Bar Failure Modes

With the cooperation of two Class I railroads, TTCI and ENSCO, Inc. conducted three field surveys of rail joints in revenue service locations on continuous welded rail (CWR) territory and bolted rail territory in 2012. During these field surveys, the survey team followed the Optical Automated Joint Bar Inspection System (JBIS) vehicle during its normal inspection runs. The team stopped at locations where the JBIS identified a defective joint. Detailed information and various measurements were collected on each joint before the repair crews removed a defective bar. Defective joint bars were collected and transported to TTC, where the fracture surfaces of the defective bars were exposed to examine the origins of crack formation (i.e. initiation). The information and measurements collected during these field surveys included:

- Location and length of crack(s)
- Markings (e.g., year, rail size, manufacturer, etc.)
- Track geometry information such as track gage, alignment, and cross level at the joint location and at a selected distance on both sides of the joint
- Track parameters such as head mismatch, tread mismatch, rail end batter, rail end gap, and estimated deflections under load
- Photographs of the joint bar
- Photographs of track condition in the vicinity of the joint

The field survey team also stopped at randomly selected intact joints to gather the same information that was collected at the defective joint locations. The information collected from intact joint bar locations was used to establish a control group, which would help identify factors that distinguish intact and failed joint locations. Moreover, a database was developed that contains information on over 100 cracked and intact joint bars.

Based on the information collected during the field surveys and the additional studies, cracks in joint bars may be classified into five different types, each with an associated mode of failure:

Top Center Crack: This type of crack initiates on the top of the joint bar, apparently at the location where the rail ends come into contact with the joint bar. Gouges from the railhead that dig into the joint bar and metal flow are associated with this type of crack. Figure 1 shows photographs of a crack at the top of the joint bar both before and after the bar was broken to expose the fracture surfaces. The mating fracture surfaces exhibit macroscopically visible ridges, sometimes referred to as clamshell or beach marks, which are characteristic of metal fatigue. Evidence of metal flow at the top of the bar can also be seen in the photograph on the right-hand side.

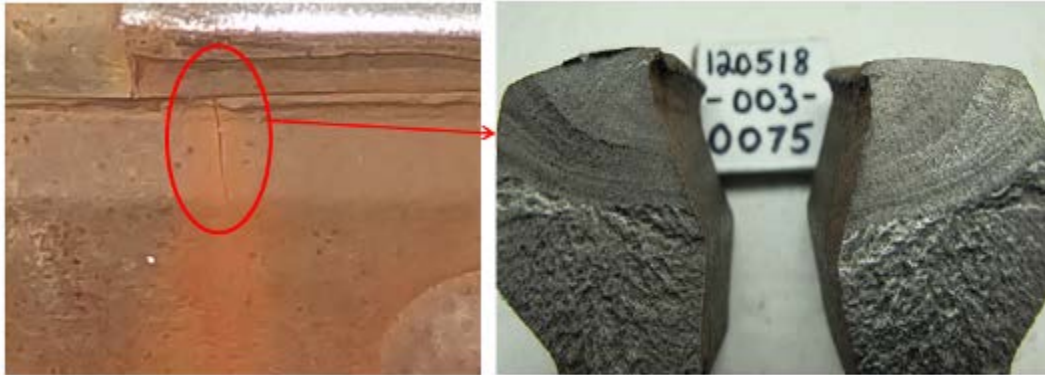


Figure 1. Top Center Crack

Joint Bar Bolt Hole Crack: Cracks may be initiated at the rough spots on the inside of bolt holes that are produced from hot punching. In other words, the stress concentration that causes this type of crack is from the fabrication or manufacturing process rather than applied wheel loading. Such cracks appear to propagate toward the bottom or top of the joint bar at an angle. Figure 2 shows photographs of a joint bar bolt hole before and after the bar was broken to expose the fracture surfaces.



Figure 2. Joint Bar Bolt Hole Crack

Bottom Center Crack: This type of crack starts from the bottom center where the joint bar makes contact with the rail base. Figure 3 also shows clamshell marks on the fracture surface of this type of crack, indicating that metal fatigue is the likely mechanism for crack initiation.

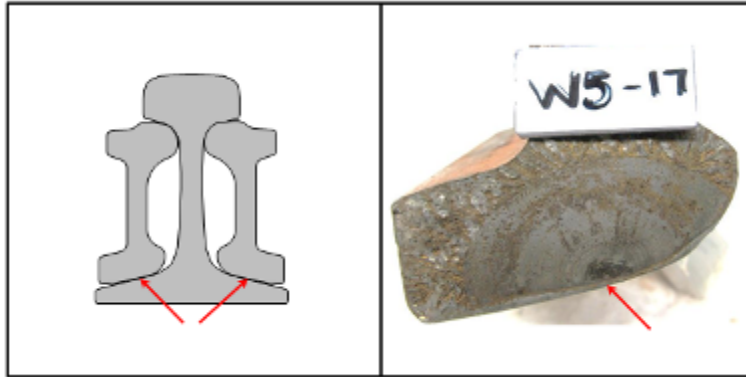


Figure 3. Bottom Center Crack

Bottom Edge Crack: This type of crack starts at the bottom edge of the joint bar. Figure 4 shows the fracture surface of this type of crack, which exhibits the beach marks that are indicative of metal fatigue. Moreover, the bottom edge location on the joint bar, which appears to be the place where the crack was initiated, coincides with the location of maximum tensile bending stress due to passing wheels.

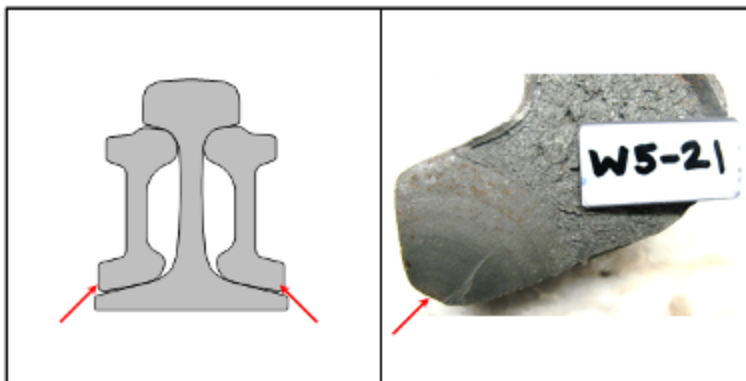


Figure 4. Bottom Edge Crack

Quarter Crack/Quarter Break: The quarter crack or break is commonly found in older types of angle bars that are longer manufactured. These angle bars have a long toe with square or rectangular holes to accommodate spikes. The corners of these spike holes are locations of high stress concentration, which leads to crack formation. Photographs of quarter defects are shown in Figure 5. The photograph on the left-hand side shows a crack emanating from the spike hole. The photograph on the right-hand side of the figure shows a crack that has propagated through the entire width of the bar, and in this case is called a quarter break.

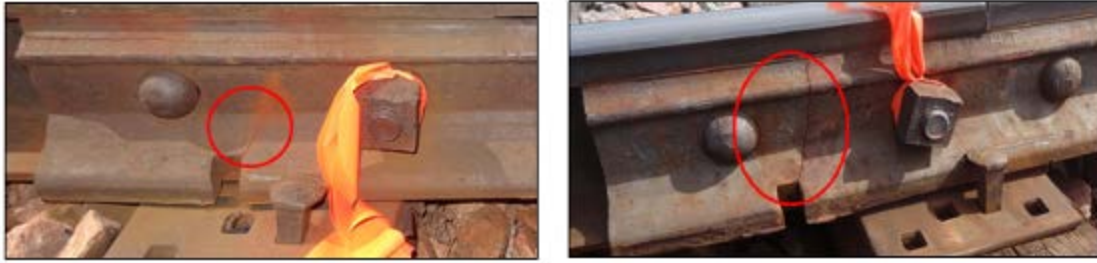


Figure 5. Quarter Crack and Quarter Break

Metallurgical analysis conducted on seven samples revealed that the microstructure of those joint bars were ferritic with a small amount of pearlite. However, no correlation was established between crack initiation and joint bar microstructure.

A review of the data collected from the field surveys and rail joints at FAST revealed that vertical deflection at the rail joint has a significant statistical correlation with intact and failed rail joints. Figure 6 shows the distribution of vertical deflections for intact and failed rail joints. Vertical deflections are grouped into ¼-in bins ranging between zero and 2 in. For example, the vertical deflections between zero and 0.24 in were measured at 20 joint locations; 18 at intact locations and two at defective or failed locations. The figure shows measurements from a total of 118 joint locations; 50 intact locations and 68 failed locations. Vertical deflections of 1.5 in or greater were measured at nine joint locations, all of which had defective or failed joint bars. Moreover, the figure shows more defective or failed joints than intact ones when the vertical deflections are ½ in or greater. At deflections less than ½ in, intact joints outnumber the failed ones.

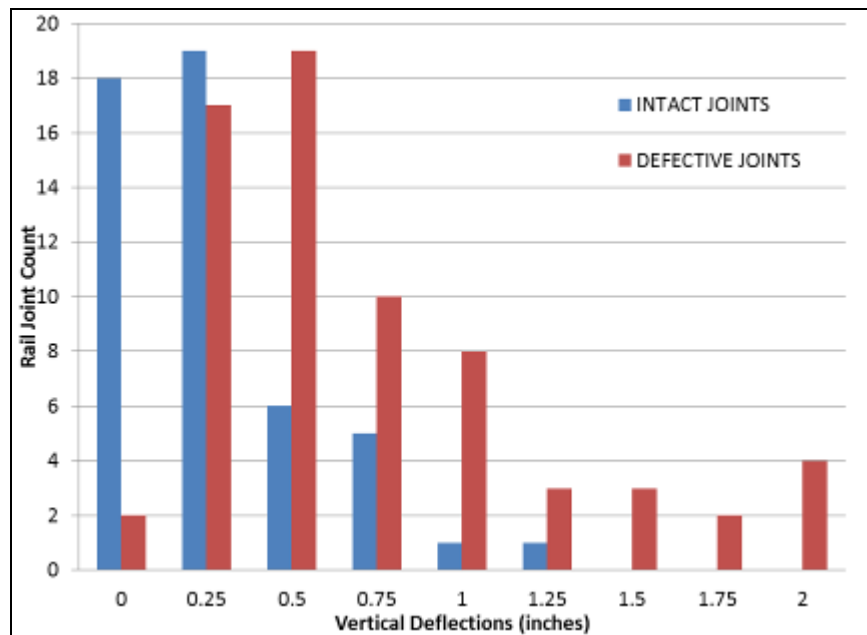


Figure 6. Distribution of Vertical Deflections for Intact and Defective Rail Joints

The data shown in Figure 6 cannot determine whether higher deflections are the cause or the effect of defective or failed joint bars. However, studies cited in the Phase I report [1] indicated that foundation deflection of the joint has a significant effect on bending stresses, which suggests that higher deflections play a role in joint bar failures.

Additional analyses of the data collected from the field surveys were conducted to examine the effects of: (1) joint movements in the lateral and longitudinal directions; (2) geometry measurements for cross level, alignment, and profile; and (3) rail end batter. The results of these analyses are summarized in Reference [3]¹.

¹ The data analyzed in Reference [3] includes information and measurements collected from other field surveys conducted by ENSCO, Inc. in addition to the surveys mentioned in this report. Additional data increases the sample size for both intact and defective rail joints, and provides further confirmation that the vertical movement at the rail joint plays a significant role in joint bar failures.

3. Effects of Track Surfacing on Joint Bar Stresses

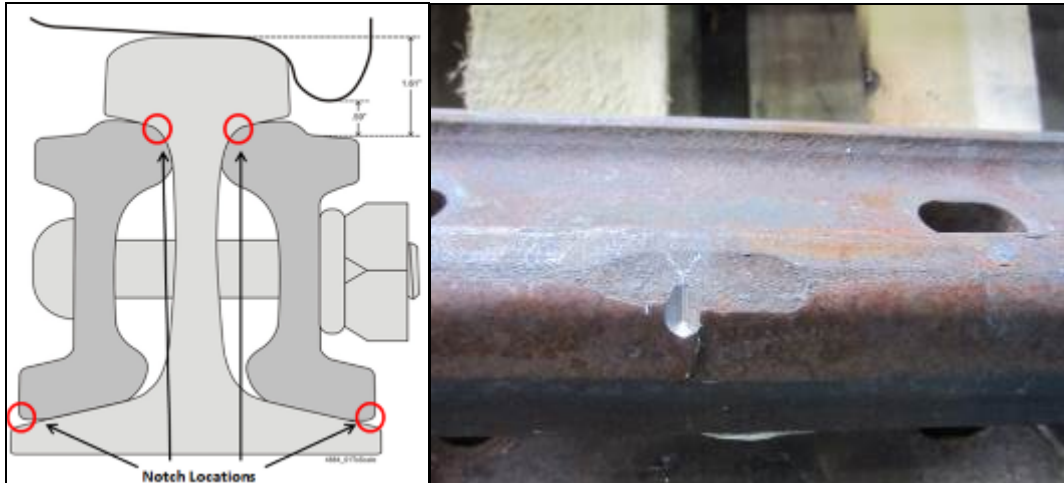
The notching of joint bars, which is induced by cyclical contact with the ends of the parent rails under traffic, is a well understood phenomena in the industry. Notches that are formed in this way can lead to the propagation of cracking or, ultimately, the failure of the joint bar entirely due to fracturing from cracks initiating at these points of contact. This study investigated the possibility of such failures resulting from regular track maintenance activities (i.e., track surfacing). Joint bars with and without notches were installed on a section of track that reflects typical settlement conditions that are seen in the revenue service environment (Figure 7). Strains from the joints bars were collected during the track lifting, and the joints bars were inspected after testing for any signs of cracking.



Figure 7. Installation of the Joint Bars in the Test Zone at FAST

3.1 Test Setup

Four standard joint bars, taken from Phase I of this study [1], were used in this investigation. Artificial notches that were approximately 0.12 in deep were machined into two of the joint bars at the top and bottom of the joint bar, as indicated in Figure 2. These joint bars were then installed in suspension (with the joints between the cross-ties) on a 5-degree curve section of track at FAST that had its ballast undercut before testing. The undercut ballast extended approximately five ties in length on either side of the joint bars (Figure 8). The two notched joint bars were grouped together on the outside (high) rail while the unnotched bars were grouped together on the inside (low) rail.



**Figure 8. Location of the Artificial Notches (left),
One of the Artificial Notches at the Top of a Test Joint Bar (right)**

Before tamping, top-of-rail (TOR) elevations were taken over the test zone and on 20 crossties on either side of the rail joints. TOR elevations were taken with and without a static load of a freight car (approximately 315,000 lb), as Figure 9 shows. Then, the ballast was replaced and tamped before another set of elevation measurements was taken under identical conditions (i.e., with and without the static load of a loaded freight car).



Figure 9. Placement of the Loaded Freight Car in the Test Zone

Bending circuits were placed at two locations on each joint bar: top and bottom along the centerline (Figure 10). Bending strains were collected on all four of the joint bars while the track was lifted to a height typically observed during regular track surfacing operations. The tamper (Figure 11) ran through the test location and performed normal surface and lining operations,

which consisted of (1) lifting of the rail (three times to approximately 1 in), (2) tamping the ballast underneath the cross-ties, and (3) ensuring the proper alignment of the rail.

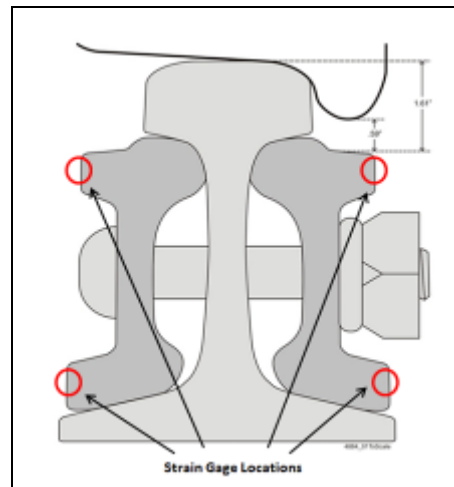


Figure 10. Location of Bending Circuits along the Central Axis



Figure 11. Tamper Used to Complete Surfacing Operations at FAST for this Study

3.2 Results and Discussion

Figure 12 shows the results of the TOR elevations before tamping operations for both loaded and unloaded scenarios, while Figure 13 shows the corresponding results after tamping operations for the loaded and unloaded scenarios.

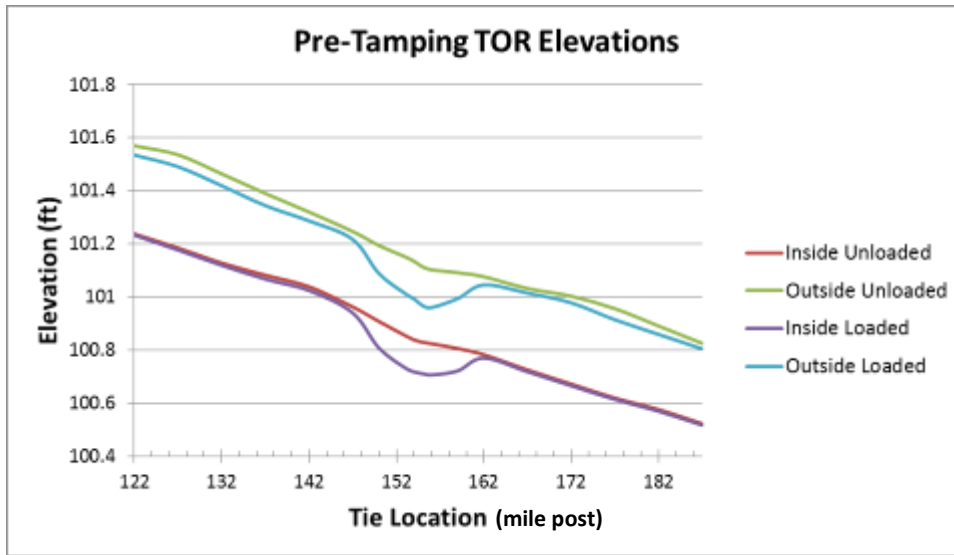


Figure 12. Plot of the Pre-Tamping TOR Elevations for the Test Zone, for both Loaded and Unloaded Scenarios

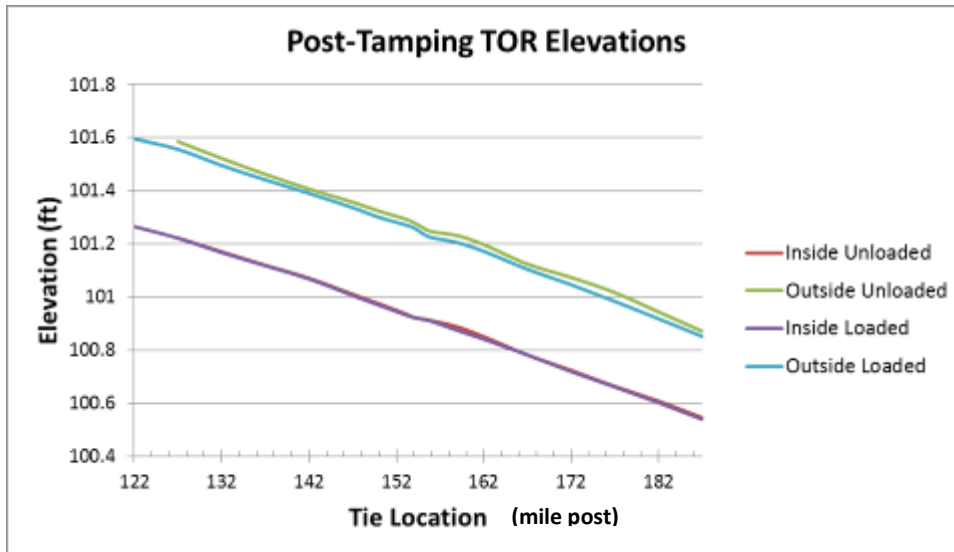


Figure 13. Plot of the Post-Tamping TOR Elevations for the Test Zone, for both Loaded and Unloaded Scenarios

In both figures, the lines slope downward as the crosstie location number increases, due to the downhill grade at the test location. Before tamping, both the inside and outside rails dip slightly under the weight of the loaded freight car, showing the amount of bending experienced by the joint bar. Over the newly tamped ballast, elevations appear to be consistent between the test area and the adjacent sections of track. Post-tamping TOR elevations show little to no difference between the loaded and unloaded conditions, which suggests there are added benefits to ensuring stiff ballast conditions via regular track substructure maintenance (which prevents additional bending of joint bars under traffic).

Bending strains were collected before, during, and after the tamping of the ballast underneath the test section at FAST. During the lifting, the top of the joint bar primarily experienced tension while the bottom of the joint bar experienced compression, as Figure 14 shows (which presents the strain output for two joint bars during surfacing). In general, the maximum bending stresses observed during the testing occurred while under the load of the tamper wheel, which notably exceeded the stress experienced by the joint bars due to the lifting of the track.

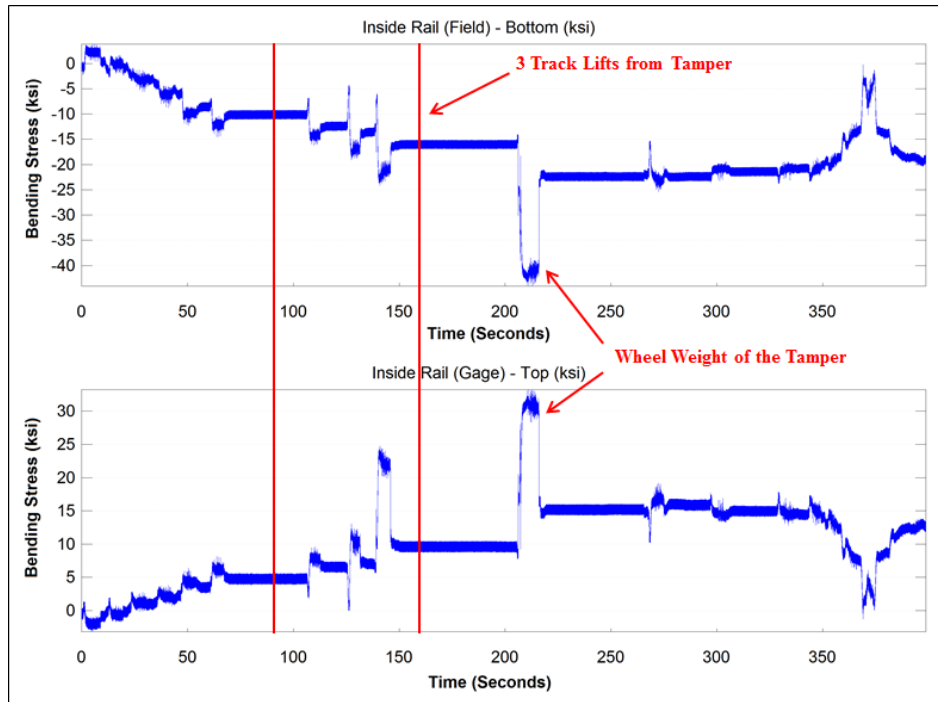


Figure 14. Stripcharts Presenting the Bending Stresses for Two of the Four Joint Bars

Two joint bars (i.e., from the inside (low) rail joint bars, field and gage sides) have bending stress values larger than those experienced within the track lifting zone (see Figure 14); the maximum compressive and tensile stresses occur from the wheel load of the tamper. The weight of the tamper wheel is approximately 17,500 pounds. The maximum compressive bending stresses from track surfacing occurs at the top of the gage side joint bar on the inside (low) rail under wheel weight, with a value of approximately 33.23 ksi (thousand pounds per square inch). Also, the maximum tensile bending stresses occur at the bottom of the field side joint bar on the same rail, also under the wheel weight, with a value of approximately 44.06 ksi. Excluding the wheel load of the tamper, the maximum bending stresses occurs at the bottom of the notched field side joint bar on the outside (high) rail, with a value of 31.75 ksi (tensile). In comparison, the maximum observed value for the unnotched joint bars was 23.68 ksi (i.e., bottom of the gage side joint bar on the inside or low rail).

A study conducted by TTCI in 2006 found that the bending stresses of insulated joint bars in revenue service have maximum values less than 45 ksi, well below the nominal yield strength of the joint bar (i.e., 70 ksi) [4]. All tensile stresses measured during the testing at FAST, including those observed under the wheel load of the tamper, were below 70 ksi.

The largest amount of bending stress in the joint bars was observed under the wheel weight of the tamper, so it is unlikely that periodic tamping associated with track surfacing operations is a factor in causing excessive fatigue of joint bars in revenue service. There was not a noticeable difference between the reaction of the notched and unnotched joint bars during the tamping operations, although it appears the wheel load from the tamper was insignificant with regard to the bending stresses observed. Nondestructive examination (NDE) was conducted on the joint bars following the testing at FAST; no defects were reported in any of the joint bars.

4. Effects of Bolt Torque Loss on Joint Bars

The data collected in Phase I shows that bolts with lower torque typically cause higher bending stresses in joint bars compared to those with higher torque [1]. However, the torque does not remain constant during the service life of joint bars. There are three primary sources of torque loss: (1) vibrations, (2) bolt relaxation, and (3) metal flow at joint bar contact locations. The first and second sources can easily be addressed by using vibration-free fasteners and by retightening the bolts periodically. However, the third source of bolt torque loss is more difficult to manage, because the tightening of the bolts increases metal flow at the joint bar/rail interface, which, in turn, causes further relaxation in the bolts. For this study, a pair of joint bars was subjected to post-hardening in order to reduce the amount of metal flow experienced by the joint bar under service conditions. This set of joint bars was then compared against the performance of untreated joint bars in identical service conditions.

4.1 Induction Hardening of Joint Bars

Many steels can be hardened by an induction-based hardening process. A large alternating current passes through a coil to generate a magnetic field, and the bar is placed within the magnetic field. The joint bar is heated as the current flows. To be hardened, the steel must be heated above its transformation temperature, which is approximately 1500 to 1800 °F (i.e., 815 to 980 °C), then rapidly quenched. The penetration depth in the work piece is inversely proportional to the frequency, so this process can harden specific areas of a part near the surface and, in turn, minimize distortion.

For this project, two joint bars were induction hardened to reduce the wear at the joint bar and rail interface. The joint bars were induction hardened in the areas shown in Figure 15 to a depth of approximately 1 in. The induction heat treatment was applied only to the middle 16 inches of each bar because that area is in contact with the bottom of the railhead. The joint bars selected had an initial hardness of approximately 300 Brinell Hardness Number (BHN). The desired hardness in the hardened section is between 410 and 450 BHN.

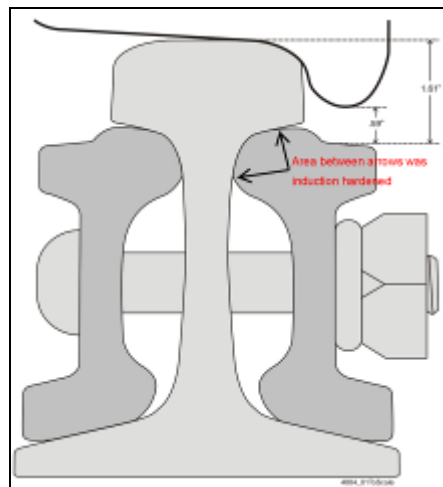


Figure 15. Locations of the Induction Hardened Areas on the Joint Bars

4.2 Test Setup

A set of six measurement locations were established on two sets of standard joint bars (i.e., a pair of post-hardened bars and a pair of untreated bars). These locations (red area in Figure 16 and close-up photograph in Figure 17) allow for pre- and post-test comparisons to determine if there was a reduction in metal flow, which could potentially aid in the preservation of bolt torque in revenue service.

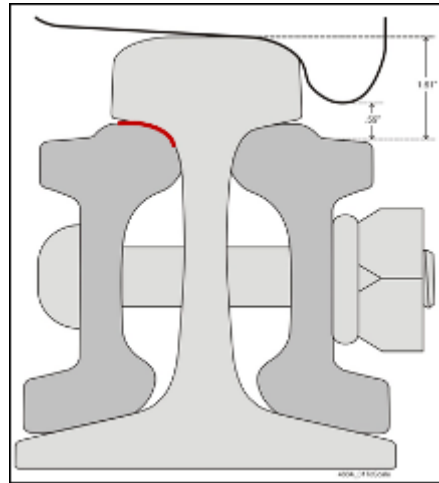


Figure 16. Diagram Noting the Location of Longitudinal Profile Measurements



Figure 17. Longitudinal Profile Measurement Locations at the Top of a Test Joint Bar

Before installation, baseline longitudinal profile measurements were taken on all four of the joint bars with a portable electronic profile measurement device. Next, the joint bars were installed in suspension on a tangent section of track at FAST and subjected to 55 MGT of HAL traffic over the course of five months. The two post-hardened joint bars were installed on the field side of the outside and inside rails, while the untreated bars were installed on the gage side of the rails. Four bolts were installed on each set of joint bars, as Figure 18 shows, and tightened to 600 ft-lb of torque. A second and final set of measurements were gathered after the joint bars were removed from the track.



Figure 18. Installation of Standard and Post-Hardened Joint Bars at FAST

4.3 Results and Discussion

After 55 MGT was accumulated at FAST, the joint bars were removed. Longitudinal profiles of the joint bars were taken and compared against the profiles made at the start of testing. The comparison revealed a buildup of metal flow adjacent to the easement at the top of the joint bars; there were differing amounts of metal flow between each of the joint bars, but there did not appear to be a distinguishable difference between the joint bars treated with the induction hardening process and the untreated joint bars. Figure 19 shows the longitudinal profiles in the area of metal flow for all of the test joint bars, while Figure 20 shows photographs of the metal flow areas (outlined in red) for an untreated and a post-hardened joint bar.

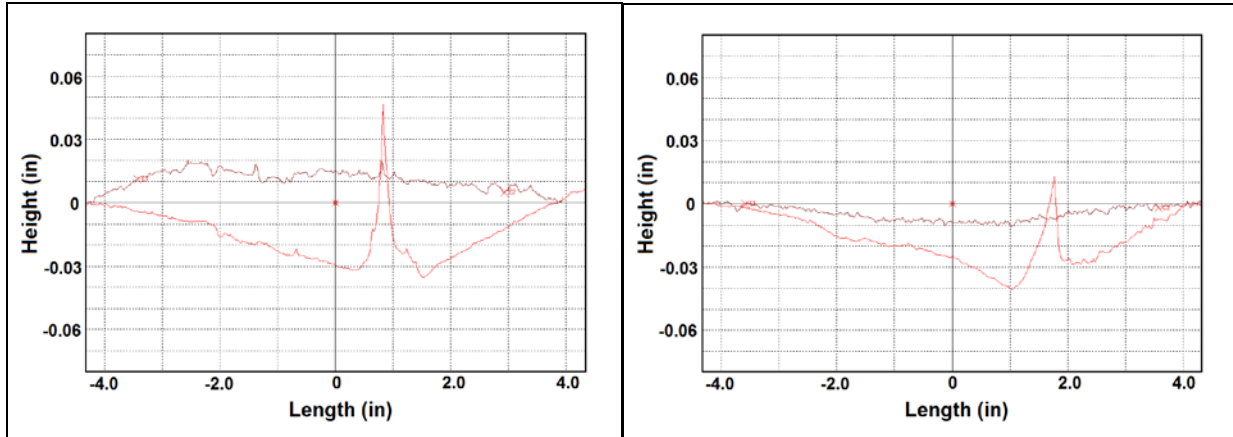


Figure 19. Pre- and Post-Test Longitudinal Profiles for an Untreated (left) and a Post-Hardened (right) Joint Bar



Figure 20. Post-Test Metal Flow for an Untreated (left) and a Post-Hardened (right) Joint Bar

Results have been interpreted qualitatively, because the permanent bending of the joint bar did not allow for an adequate reference that could provide accurate quantitative information on the amount of material accumulated adjacent to the easement. Photos taken following the joint bar's removal from the track (see Figure 20) show contact was primarily focused in the area on top of the joint bar, just above the easement, where the bottom of the railhead makes contact with the top of the joint bar. The easement is partially filled with material from areas outside the easement, leading to more contact with the railhead. This condition is most likely the result of higher contact forces adjacent to the easement, which were also observed in the FEA (see Section 7). Bolt torque loss would accelerate this condition by amplifying the bending, resulting in more contact with the railhead.

During the in-track testing, cracks began to form on an untreated and a post-hardened joint bar (Figure 21), which emanated from the bottoms of the joint bars and progressed upward (under the center-left bolt hole in the untreated bar and at the midsection in the post-hardened bar). Both joint bars were removed from track before the cracks reached the bolt holes.



Figure 21. Fatigue Cracking in an Untreated (left) and a Post-Hardened (right) Joint Bar

5. Effects of Railhead Gaps and Mismatches on Joint Bars

The use of temporary joint bars in CWR territory may create some of the problems that were common during the era of jointed rail. The rail gap between jointed rails, typically observed to be approximately $\frac{1}{4}$ in, may result in higher impacts and metal flow at the ends of the railhead as well as the batter at the ends of the jointed rails. Theoretically, higher gaps at the rail joints can cause increased wheel impact forces and, in turn, accelerate foundation deterioration. This study evaluates the benefits of “no gap” joints using larger diameter bolts and higher torques against those with gaps up to 1 in. Larger diameter bolts and higher torques may help to “freeze” the joints and prevent further development of a gap between the parent rails. This, in turn, should aid in reducing the wheel impact forces at joints.

In a similar way, the jointing of rails with differing profiles may result in higher wheel impact forces and metal flow due to railhead mismatch. These wheel impact forces may likely result in increased bending stresses in the joint bars and, due to the tread mismatch, those that may not directly affect the center axis of the joint bar where bending stresses are normally highest. This study also investigates the effects of railhead mismatch under the same wheel loads.

5.1 Test Setup

Four standard 132-pound joint bars were instrumented with strain gages along the central axis (recall Figure 10). These joint bars were then installed in suspension on a tangent section of track at FAST (see Figure 22), joining the parent rails with two short plugs, one on each rail (i.e., outside and inside). Both joints were located across from one another, offset by two crossties. These short plugs were joined to the adjacent parent rail, using the test bars on the west end and standard bars on the east end of each plug. This configuration allowed the gap to be easily adjusted for the differing gap sizes, as per the requirements of testing. The gap was maintained using rail anchors to prevent movement of the plug rail underneath the test train consist. An IWS, with a static wheel load of 39,000 lb, was used to gather data on the vertical impact forces at each of the joints. Sampled at 1200 Hz and filtered at 100 Hz, the IWS allows for the continuous measurement of wheel/rail forces at the interface, namely vertical, lateral, and longitudinal forces with a valid upper frequency of approximately 600 Hz. Wheel/rail forces and bending strain data (with a sampling rate of 512 Hz) were collected from both pairs of joints for 0-, $\frac{1}{2}$ -, and 1-in gaps at 10, 25, and 45 mph (clockwise (CW) and counterclockwise (CCW) movements). It should be noted, however, that due to the winter weather conditions at the time of testing, the gap could not be fully closed for the 0-in test runs, resulting in a gap approximately $\frac{1}{8}$ -in wide.



Figure 22. Installation of Instrumented Joints Bars at FAST

An identical approach was used to evaluate the bending stresses and vertical impact forces for differing railhead mismatch configurations. Four standard 119-pound joint bars were instrumented with setups that were identical to the bars used in testing rail gaps and installed at the same locations, which placed the joint bars across from one another and offset by two cross-ties. The gap was maintained at $\frac{1}{4}$ in using rail anchors on the plug rail. Shim plates were used to adjust the height of the parent rail to the mismatch sizes outlined in the test plan (i.e., $\frac{1}{4}$ -, $\frac{3}{16}$ -, $\frac{1}{8}$ -, and 0-in mismatches). Figure 23 is a plan view of this setup. IWS and bending strain data was collected from both pairs of joint bars at 10 and 25 mph for the $\frac{1}{4}$ - and $\frac{3}{16}$ -in mismatches, respectively, and at 45 mph for 0- and $\frac{1}{8}$ -in mismatches (CW and CCW movements).

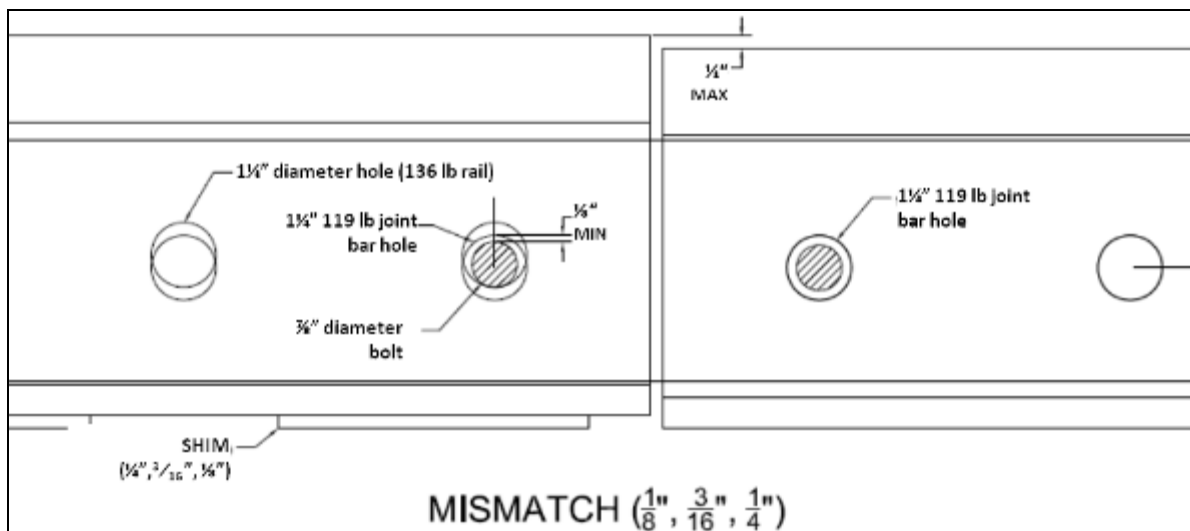


Figure 23. Plan View of an Example Railhead Mismatch Test Setup (1/2 in)

5.2 Results and Discussion

5.2.1 Vertical Impact Forces on the Joint Bars

Figure 24 shows plots of the 95th percentile of the vertical force responses, gathered over a range of 30 ft (an offset of 15 ft on either side of each rail joint was used) and collected on the differing rail gaps, namely left wheel of axle #1 (VL1) and right wheel of axle #2 (VR2). From the results collected by the IWS at the location of the two sets of joint bars, there appears to be a relationship between speed of the train consist through the test zone and the vertical force response (i.e., increased speed results in an increased vertical wheel force). However, it does not appear that there is a consistent difference between CW and CCW movements. Figure 25 is a time history of the IWS vertical wheel force data, which does not show distinguishing patterns that separate the test zone from the remainder of the section at FAST. The vertical wheel forces within the test zone do not appear to differ significantly from those in the surrounding track.

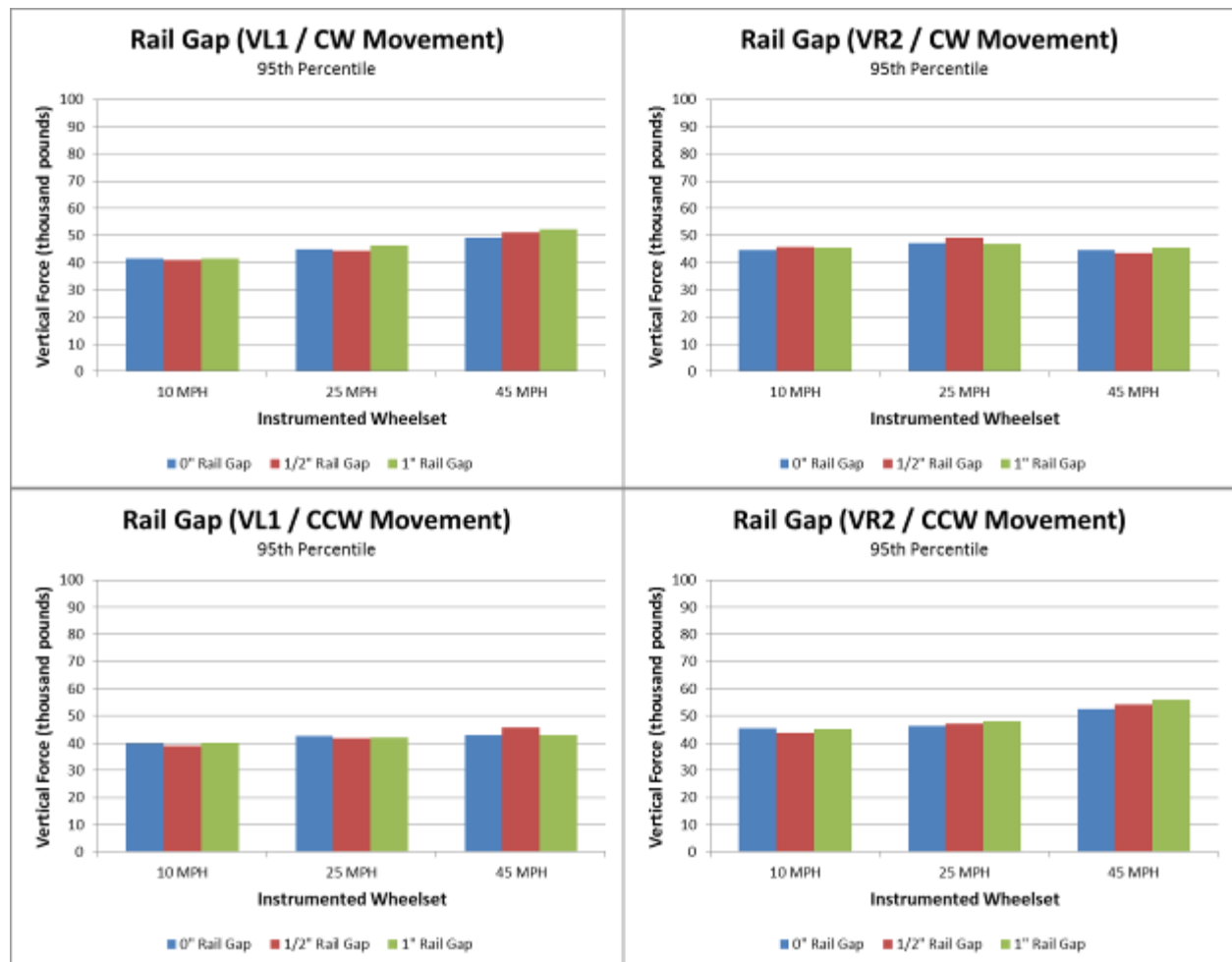


Figure 24. Plots of the 95th Percentile for IWS Vertical Wheel Force Data (Rail Gaps)

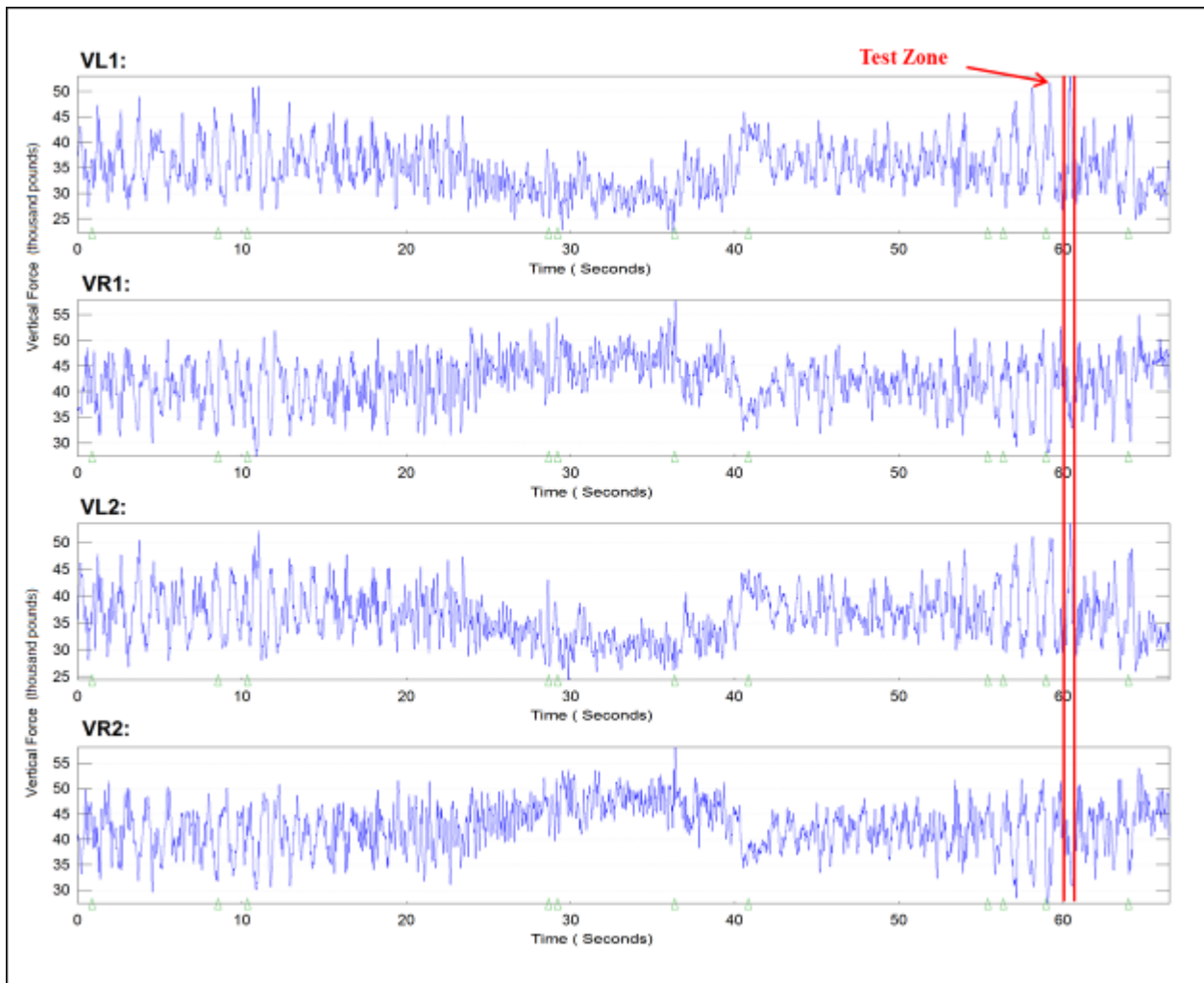


Figure 25. Time History for IWS Vertical Wheel Force Data (1-in Gap, 45 mph)

Figure 26 presents plots of the 95th percentile of the vertical force responses, gathered over a range of 30 ft (an offset of 15 ft on either side of each rail joint was used) and collected on the differing railhead mismatches. From the results collected by the IWS at the location of the two sets of joint bars, there is a definitive relationship between the speed of the train consist through the test zone and the vertical force response (i.e., increased speed results in an increased vertical wheel force), albeit all less than 60,000 lb. Although, it does not appear that any distinct conclusions can be made with regard to CW and CCW movements. As with the varying rail gaps, the vertical wheel forces within the test zone do not appear to differ significantly from those in the surrounding track (see Figure 27).

Vertical force responses were expected to be much higher than the values actually collected during the tests. Following a thorough review of the testing parameters, it is possible that the expected events at the rail joints were not captured due to inherent limitations in the IWS.

Furthermore, since this short-term test was completed in two days with newer components, the results do not reflect conditions in revenue service (where joint bars with significant accumulated

tonnage are subjected to similar loads). Also, environmental conditions at the time of testing may have influenced the results. On-track testing was completed under extreme cold weather conditions, with temperatures as low as -10 degrees Fahrenheit during the two-day testing period. Rail anchors were placed on the shorter plugs to prevent unwanted movement under the train consist.

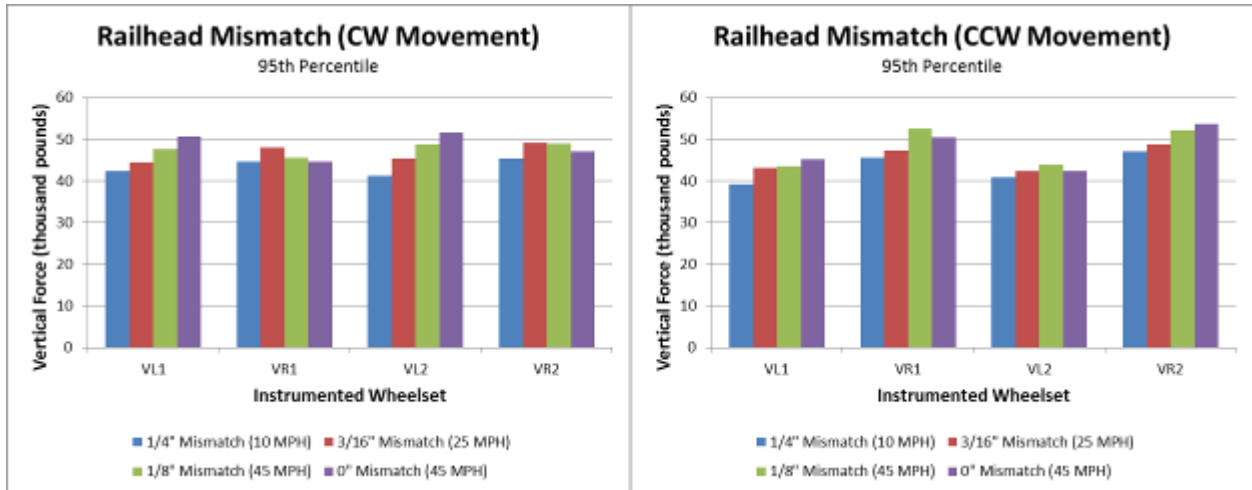


Figure 26. Plots of the 95th Percentile for IWS Vertical Wheel Force Data (Railhead Mismatch)

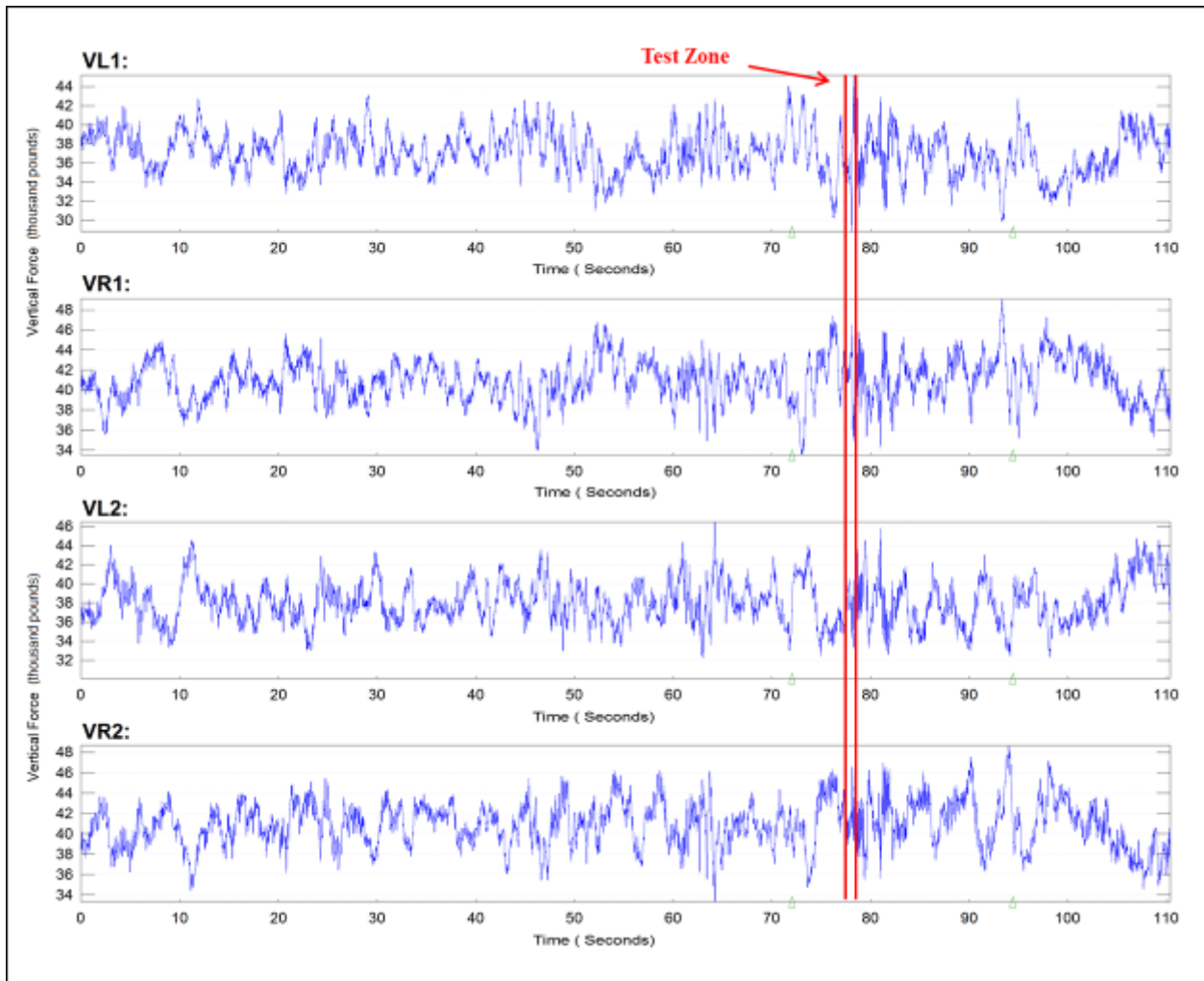


Figure 27. Time History for IWS Vertical Wheel Force Data (1/4-in Mismatch, 10 mph)

5.2.2 Bending Stresses on Joint Bars

Bending stresses collected from the strain gages were fairly consistent with what was expected from standard joint bars in revenue service. Figure 28 shows box plots of the bending stresses, based on strain gage measurements, under the passage of the 39,000-pound wheel loads. The figure shows the compressive bending stresses at the top of the joint bar and the tensile bending stresses at the bottom. The magnitudes of these bending stresses are consistent with those observed in the Phase II report [2]. However, there does not appear to be a significant difference between bending stresses for gaps at 1 in or less.

Although, it does appear that the distributions of each vary slightly between the two configurations; while the smaller gaps are more normally distributed between the 25th and 75th percentiles, those with larger gaps tend to be skewed toward higher states of either compression or tension, depending on the location of the strain gage.

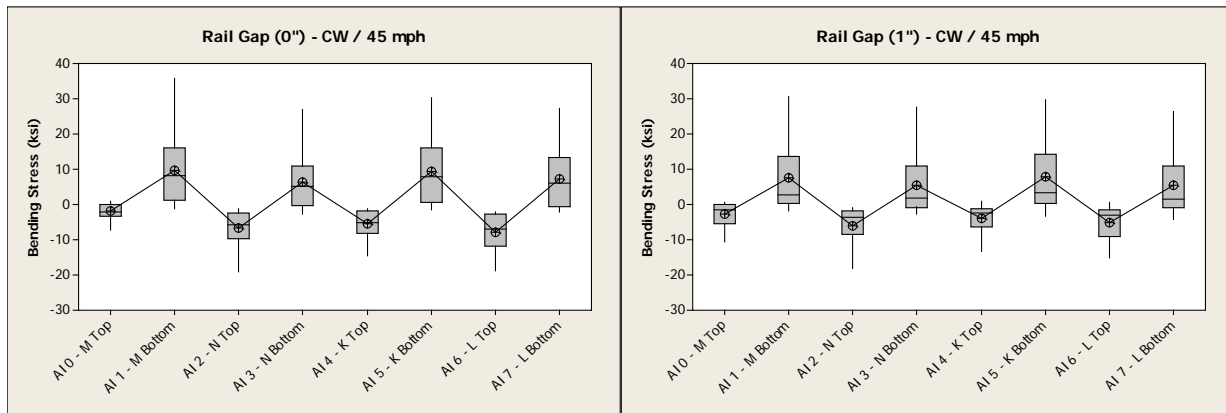


Figure 28. Box Plots of the Bending Stresses under the IWS for Each Circuit (Rail Gap)

By comparison, the bending stresses in rail joints with varying railhead mismatches differ greatly from those in joints with gaps. As Figure 29 shows, even though the bending stress are notably below 20,000 pounds per square inch for both compressive and tensile states, the joints bars are dominantly in compression under the passage of the 39,000-pound wheel loads.

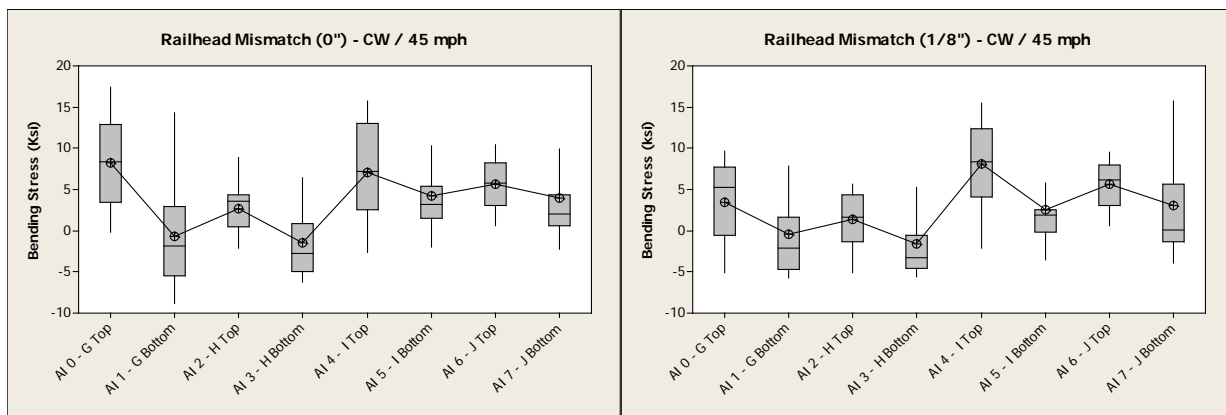


Figure 29. Box Plots of the Bending Stresses under the IWS for Each Circuit (Railhead Mismatch)

These results suggest that the test scenarios for the railhead mismatch may not represent the situation observed in the revenue service environment, in which a parent rail with a worn profile would be jointed with a relatively newer plug rail. On the contrary, as shim plates were used to elevate the parent rail to produce the required mismatches, the scenarios appear to have mimicked a situation in which there is a discontinuity in elevation of the parent and plug rails. From an engineering standpoint, this could be because (1) ballast deteriorates at a faster rate under the parent rail than that of the plug rail, or vice versa; (2) the joint bar is suspended between timber and concrete crossties, producing varying track stiffness across the length of the joint bar; and/or (3) deterioration of the rail seat on one of the crossties over which the joint bar is placed. The stress may be transferred elsewhere (e.g., bolt holes) in this situation. Depending on where the stress is transferred, the service life of the joint bar could be reduced.

6. Metal Flow versus Crack Propagation in Joint Bars

Machine vision and ultrasonic inspections systems have revolutionized the industry by providing a means to quickly and efficiently inspect joint bars in track at walking speeds or greater. This allows track inspectors to cover more miles in less time without dramatically affecting the quality of the inspection.

These systems are capable of detecting large cracks or fractures within specific areas on the joint bar. Machine vision detects cracks that are visible on the surface of the joint bar, while ultrasonic inspection aids in the detection of cracks in the top inside surface of the joint bar (which are often missed through visual inspection). There is always the possibility some cracks will go unnoticed by both systems during an inspection.

This study's goal is to determine if a correlation exists between the amount of metal flow and the propagation of cracking in joint bars. If such a correlation exists, it would provide the industry with a potential acceptance (i.e., fit for service) criterion for re-use of joint bars in track.

Discovering evidence of a relationship between metal flow and crack propagation would allow the railroad industry to develop recommendations for the amount of metal flow allowed in a joint bar before it is removed from service.

6.1 Test Setup

One hundred samples were collected from both revenue service and at TTC (80 joint bars were temporarily donated by a western railroad and 20 were collected from onsite trackage at TTC). Information on material flow and hardness was collected on all samples, then TTCI's NDE team performed computed radiography on all samples and determined whether there was a correlation between the metal flow and propagation of fatigue cracking. The inspection area of the joint bars focused on high-stress concentration locations between the center bolt holes and the head of the joint bar (Figure 30).



Figure 30. Area of Interest/Stress Concentration Location

6.2 Results and Discussion

Table 1 lists a broad range of hardness values and material flow collected from 14 samples. The range of hardness measurements is between 225 and 342 BHN, while the corresponding range of measurements for flow height fall between 0.031 and 0.125 in.

Table 1. Subset of Joint Bar Samples

Sample	Hardness (BHN)	Flow Height (in)	Type	X-Ray
1	342	0.093	No Data	No Indications
2	258	0.109	132–136 RE Std.	No Indications
3	225	0.046	132–136–141 RE Std.	No Indications
4	270	0.031	136 RE	No Indications
5	255	0.078	115 RE	No Indications
6	260	0.031	132 RE	No Indications
7	250	0.046	No Data	No Indications
8	272	0.093	132 RE	No Indications
9	239	0.031	132 RE	No Indications
10	259	0.031	132 RE	No Indications
11	253	0.062	132 RE	No Indications
12	247	0.062	132 RE	No Indications
13	263	0.125	115 RE	No Indications
14	273	0.093	115 RE	No Indications

The results of this test show no correlation between the metal flow and growth of fatigue cracking in the joint bars sampled.

There was little correlation between joint bar surface hardness and metal flow depth at the top center of joint bars, as Figure 31 shows. Surface hardness was used as a proxy for the presence of a notch (stress raiser) likely to cause joint bar cracking, because too few joint bar samples had cracking. The lack of hardness and flow depth correlation suggests that a simple measure of flow depth cannot yet be used to reject joint bars from re-using them in track. A larger sample of joint bars, including more cracked bars, is needed to reach a definitive conclusion.

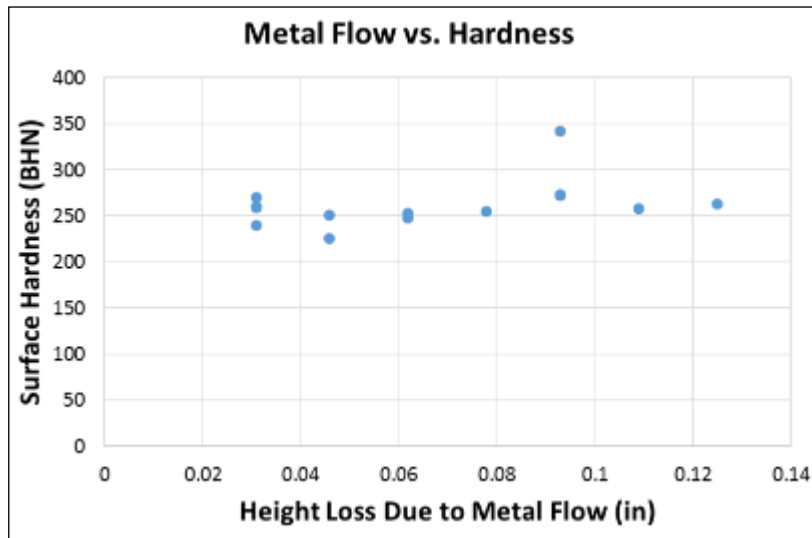


Figure 31. Plot of the Height Loss Due to Metal Flow against Surface Hardness

7. Finite Element Analysis of Bolted Rail Joint

FEAs are used to examine the structural performance of rail joints under various loading and tie-ballast conditions.² The primary purpose of these analyses is to help interpret and understand the observations and measurements from the field surveys on revenue service track and the test results from the various experiments conducted at TTC. In this section, results from the FEAs are presented to show: (1) the vertical deflection behavior at supported versus suspended rail joints, (2) the effect of bolt pattern (i.e., number of bolts and placement of bolts when only four out of six holes are bolted) on joint structural behavior, and (3) the effect of easement on contact pressures between the rail and the joint bar.

In terms of structural performance, rail joints are thought to be weak links because the section properties (i.e. cross-sectional area and area moment of inertia) are typically less than those for the rail itself. Table 2 lists the section properties for 136 RE rail and the properties for standard joint bars associated with 132 RE rail. That is, joint bars originally dedicated to join 132 RE rail are often used to join 136 RE and 140 RE rail sections.

Table 2. Summary of Section Properties for 136 RE Rail and 132 RE Joint Bars

		Cross-sectional Area, A (in ²)	Moment of Inertia, I_{yy} (in ⁴)
Rail		13.32 ^(a)	94.2 ^(a)
Short-toe Joint Bars*		11.78 ^(b)	32.28 ^(b)

NOTES:

* Properties for two bars

^(a) From Foster Rail Catalogue

^(b) From 1999 AREMA *Manual for Railway Engineering*

² The development of finite element models for bolted rail joints is an ongoing and separately FRA-funded activity at the Volpe Center. Results from the tests conducted by TTCI are used to validate the finite element modeling. Many of the finite element results presented in this report are also discussed in Reference [5].

Figure 32 shows schematic diagrams for the setup of two finite element models used for present analyses; one for a supported joint in which a cross-tie is located at the center of the joint and another for a suspended joint in which the span of the joint rail joint is centered between two cross-ties. In both models, brick elements are used to represent the rail and joint components (e.g., joint bar and bolts) in the vicinity of the joint, while beam elements are used to represent the rail away from the joint.

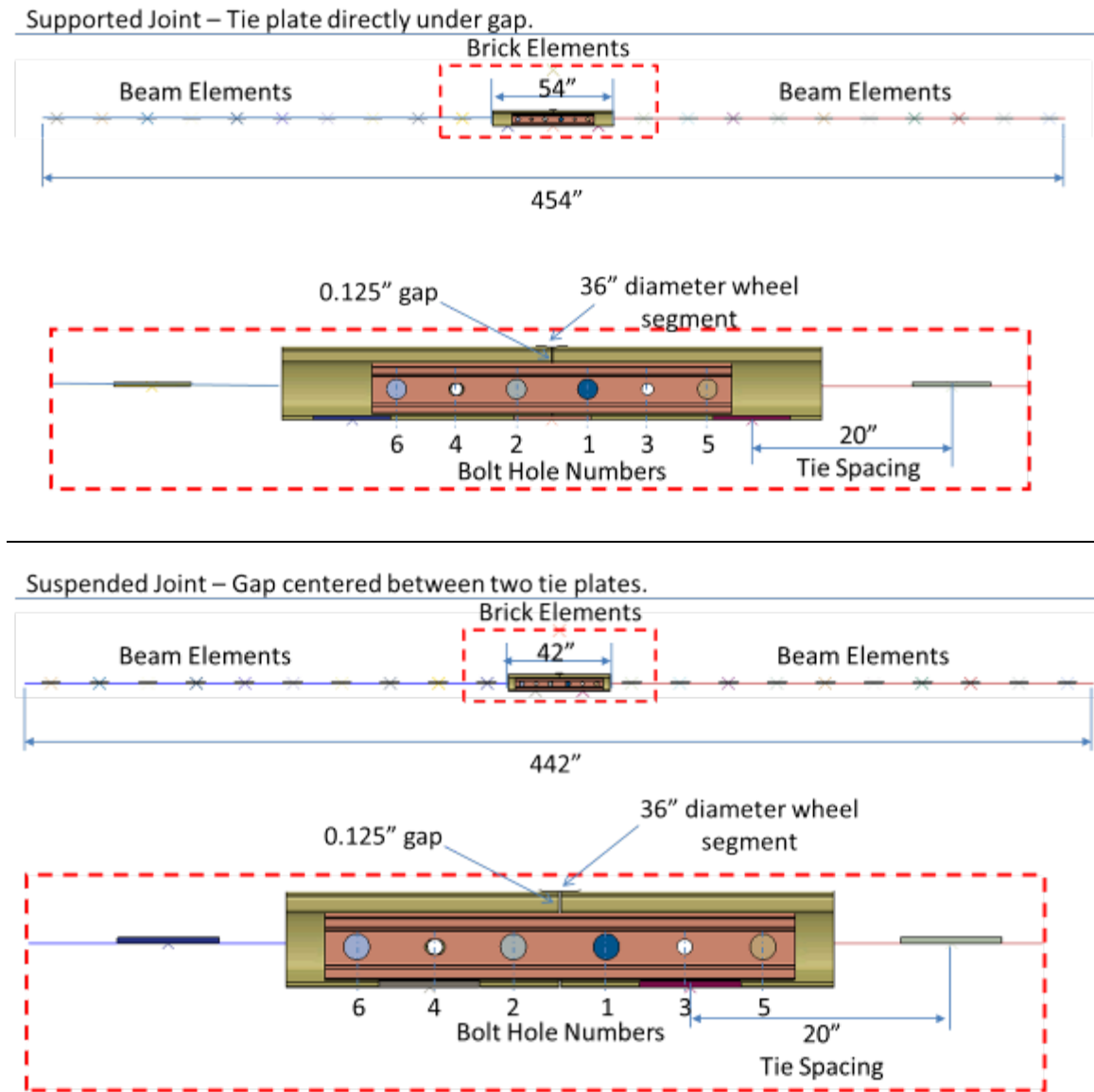


Figure 32. Finite Element Model Setup for Supported and Suspended Joints

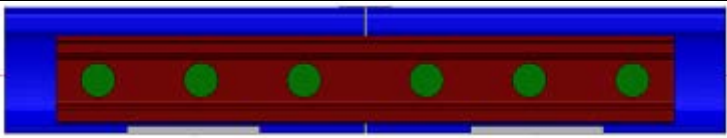
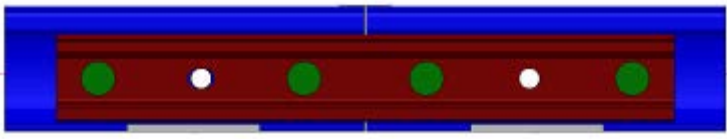
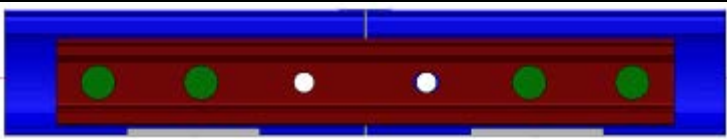
Table 3 lists the various assumptions used for tie-ballast support variables such as nominal spacing between cross-ties, linear spring stiffness, and applied wheel load. Table 4 shows the three different bolt configurations assumed in present analyses.

Table 3. Assumptions in FEAs of Supported and Suspended Rail Joints

Rail	136 RE
Joint Bars	132 RE
Initial Bolt Tension	6,000 lb per bolt
Tie Spacing*	20 in between tie centers
Tie Spring Stiffness*	60 lb/in/tie
Wheel Load	35.75 kips (286,000-lb car assumed)

*Combination of tie stiffness and tie spacing chosen to be equivalent to 3,000 psi continuous foundation.

Table 4. Assumed Bolt Patterns

6 bolts	
4 bolts – Configuration 1	
4 bolts – Configuration 2	

Observations from the field surveys indicate that the most common type of defect found in standard joint bars is crack at the top center of the bar [3]. As discussed in Section 2, metallurgical analysis of the fracture surfaces suggests that this type of cracking is caused by metal fatigue. Another factor that contributes to cracking at the top of the joint bar is thought to be a lack of easement. In the context of joint bars, an easement is a recessed portion or depression in the bar, presumably intended to reduce the possibility of rail end contact with the top of the joint bar. Figure 33 shows the AREMA recommendation for easement in head-free joint bars [6]. If the joint bar does not have an easement, or if the easement is not properly aligned, knife-edge contact between the rail ends and the top of the bar can create an area of localized stress concentration (which can cause fatigue crack initiation).

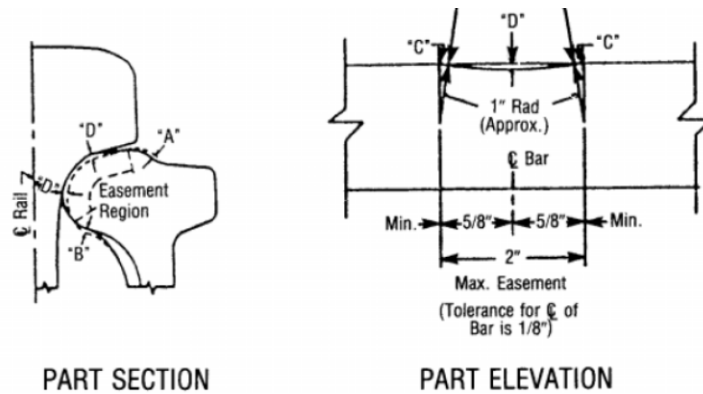
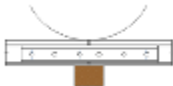
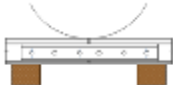


Figure 33. Recommended Head Easement for Head-Free Joint Bars [6]

Table 5 lists the magnitudes of the estimated maximum vertical deflections estimated from the FEAs for different track conditions under the nominal assumptions listed in Table 3. As noted in the table, the maximum vertical deflection for a continuous rail calculated in the FEA agrees exactly with the deflection calculated from the closed-form solution based on the theory of beams on elastic foundation [7]. Moreover, supported rail joints are shown to have smaller deflections than suspended joints. Bolt pattern has a relatively weak effect on maximum vertical deflection and Configuration 2 of the four-bolt pattern exhibits slightly larger deflections. The results also show that the easement has a relatively weak effect on vertical deflection.

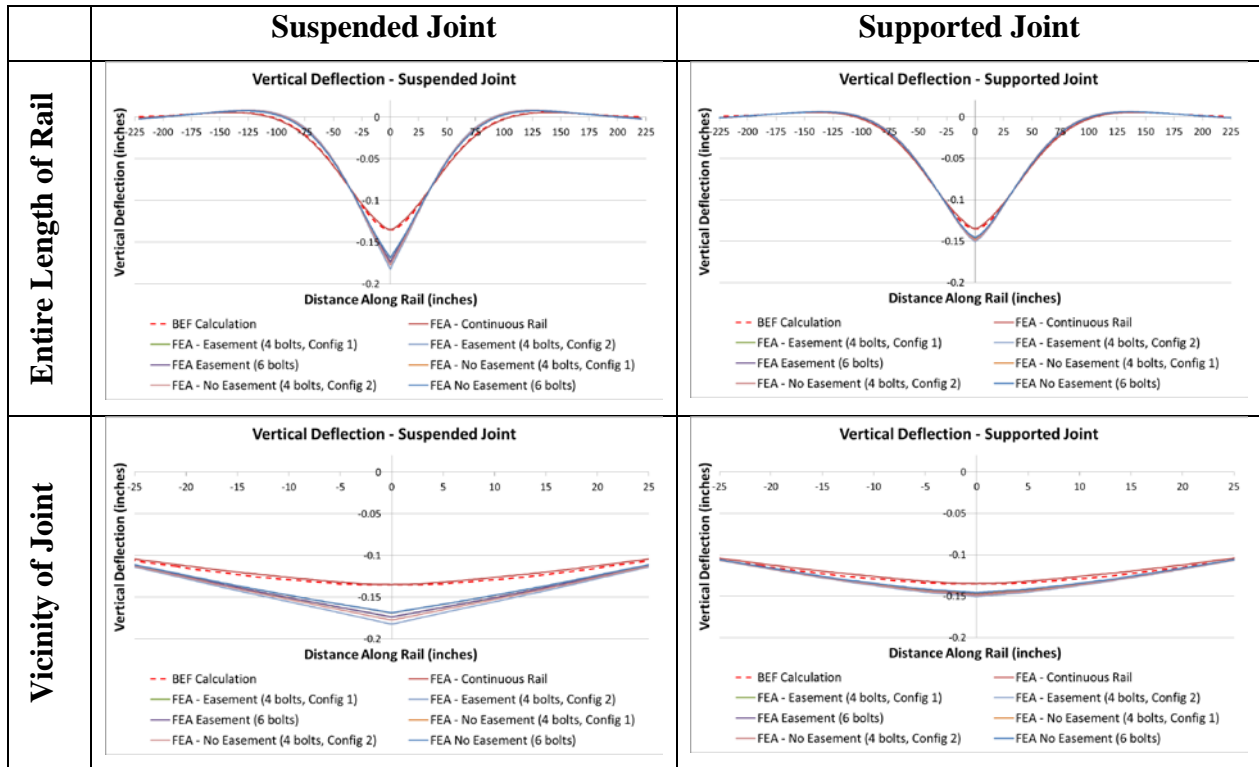
Table 6 shows how the vertical deflections vary over a longitudinal distance along the rail for the different track conditions assumed in the analyses. The table shows distributions over the entire range of track modeled in the analysis (i.e., over a 450-in span) and over a shorter range in the vicinity of the rail joint (i.e., over a 50-in span).

Table 5. FEA-calculated Deflections under 35.75-kip Wheel Load

Continuous Rail*			0.135"
Supported Joint		4 bolts Easement Configuration 1	0.148"
		4 bolts Easement Configuration 2	0.151"
		6 bolts Easement	0.148"
		4 bolts No Easement Configuration 1	0.147"
		4 bolts No Easement Configuration 2	0.149"
		6 bolts No Easement	0.146"
		Suspended Joint	
4 bolts Easement Configuration 2	0.182"		
6 bolts Easement	0.174"		
4 bolts No Easement Configuration 1	0.169"		
4 bolts No Easement Configuration 2	0.177"		
6 bolts No Easement	0.169"		

* From beam on elastic foundation theory, vertical deflection is 0.135 in for vertical wheel load of 35,750 lb.

Table 6. Vertical Deflection along Length of Rail



The effect of easement was examined by the FEA, which determined the locations of contact between rail and joint bar and estimated the relative magnitude of contact forces and pressures acting on the bar and the rail. Figure 34 shows a free-body diagram of the forces acting on a joint bar under a positive bending moment. The distance between the two distributions of pressure on the top of the joint bar are intended to represent the location where the rail ends do not contact the joint bar due to the easement. Moreover, the schematic shows the anticipated pressure distributions acting on a joint bar.

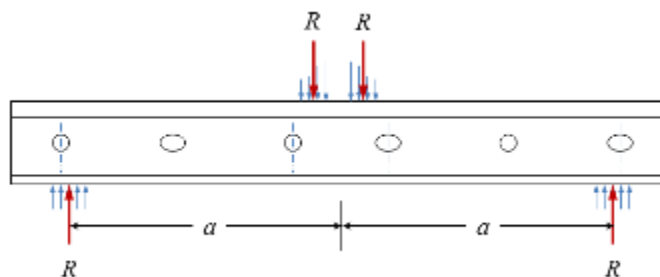


Figure 34. Joint Bar Reactions under Positive Bending

Table 7 shows the FEA's calculations of contact forces acting on standard joint bars in supported rail joints for different bolt configurations with and without easement. Similarly, Table 8 shows FEA results that correspond to a suspended rail joint. The contour plots presented in these two tables are not meant to call attention to the absolute value of maximum force, which is likely to be highly dependent on mesh size, but rather to show the relative relationship between contact area and maximum contact force for the various configurations with and without easement. That is, the reaction forces calculated by the FEA at the top of the joint bar are similar in shape (i.e. triangular) to those shown in the schematic in Figure 34. However, the FEA-calculated distributions of reactions at the bottom of the joint bar are quite different and vary depending on the bolting pattern or configuration. Moreover, the magnitudes of the contact forces are higher in suspended rail joints than those in supported joints. The total area of contact between the joint bar and the rail appears to be greater in the suspended joints. Contact forces are higher in bars without easement than in bars with easement.

Table 7. Contact Force Normal to Element Faces on Joint Bar (Supported Joint)

	<p>4 bolts Easement Configuration 1</p>		
	<p>4 bolts Easement Configuration 2</p>		
<p>CNORMF, Resultant</p>	<p>6 bolts Easement</p>		
<p>Supported Joint</p>	<p>4 bolts No Easement Configuration 1</p>		
	<p>4 bolts No Easement Configuration 2</p>		
	<p>6 bolts No Easement</p>		

Note: Maximum contour for all cases set at 1,000 lb.

Table 8. Contact Force Normal to Element Faces on Joint Bar (Suspended Joint)

<p>CNORMF, Resultant</p> <p>Suspended Joint</p>	<p>4 bolts Easement Configuration 1</p>
	<p>4 bolts Easement Configuration 2</p>
	<p>6 bolts Easement</p>
	<p>4 bolts No Easement Configuration 1</p>
	<p>4 bolts No Easement Configuration 2</p>
	<p>6 bolts No Easement</p>

Note: Maximum contour for all cases set at 1,000 lb.

Figure 35 is a schematic of the rail joint cross section that shows two locations where contact between the rail and the joint bar are likely to occur. Moreover, these locations have been identified in Section 2 as potential locations to develop or initiate cracks at the top and bottom of a joint bar.

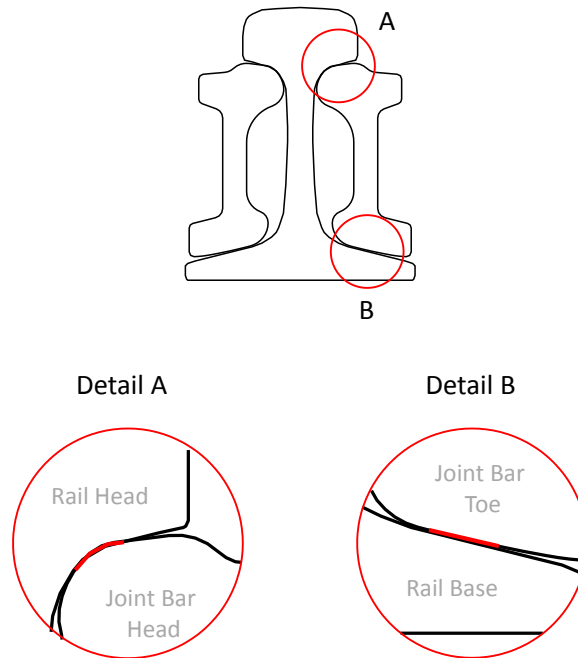
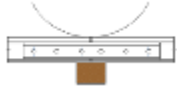
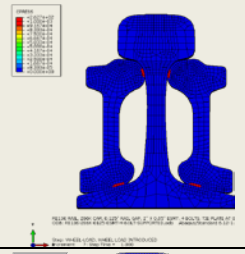
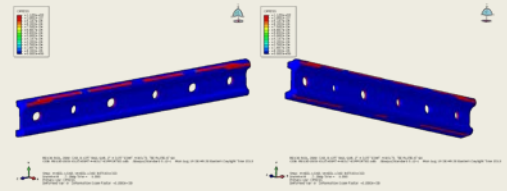
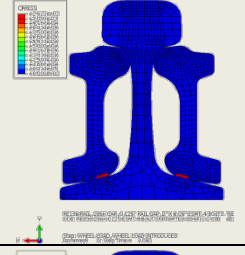
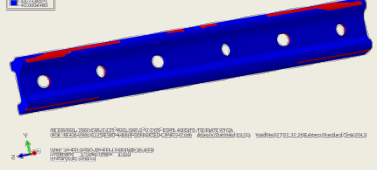
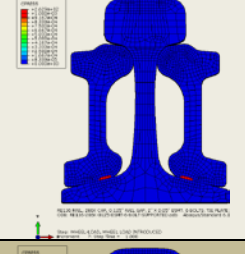
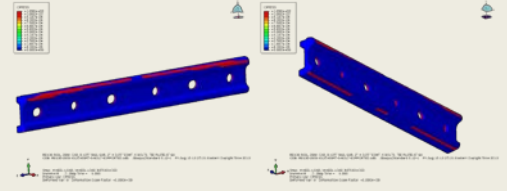
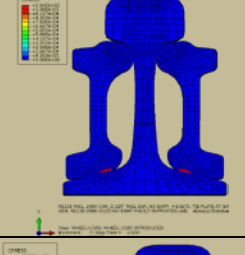
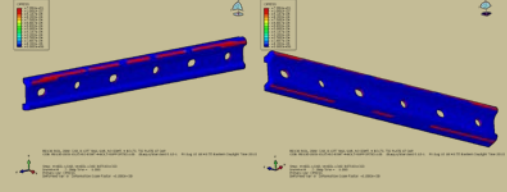
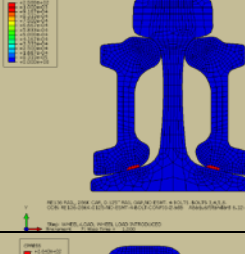
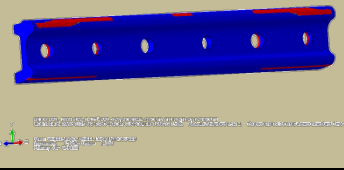
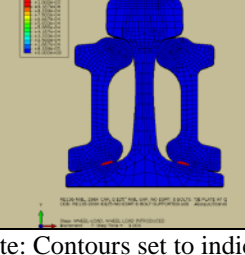
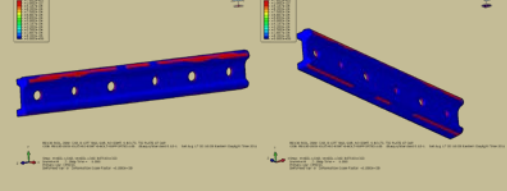


Figure 35. Potential Locations for Contact between Rail and Joint Bar

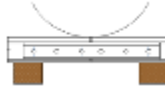
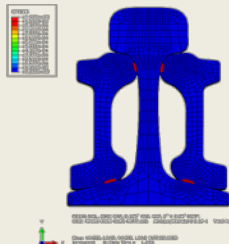
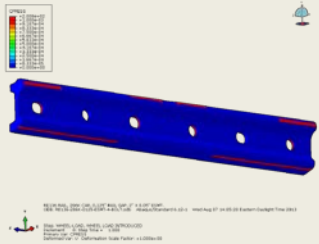
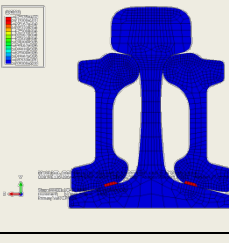
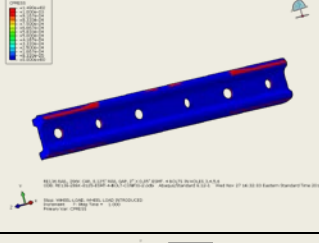
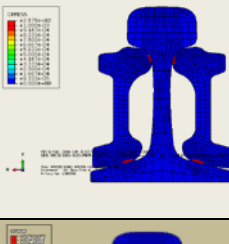
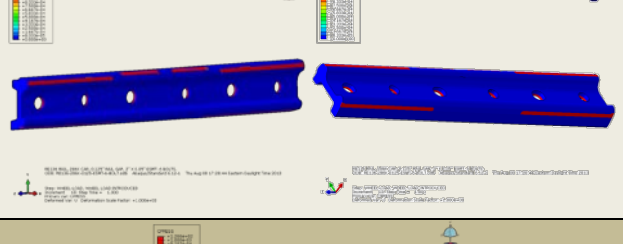
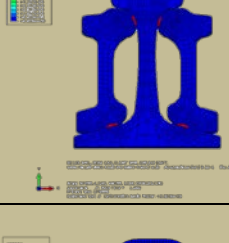
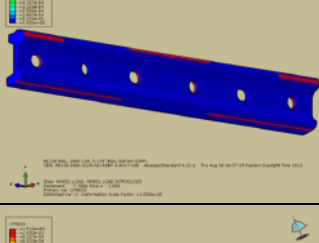
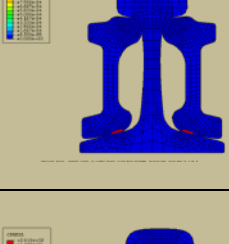
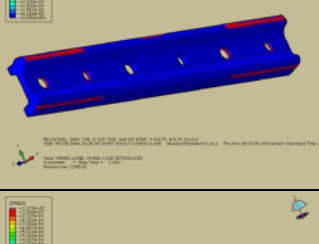
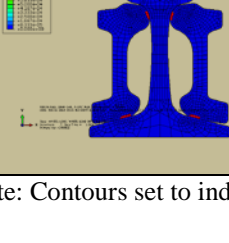
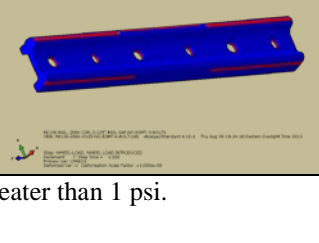
Table 9 shows contour plots where contact pressures greater than 1 psi are acting on the joint bar and the rail for a supported joint. The contact pressures are greatest adjacent to the easement. High contact pressures are likely to cause plastic flow, which may ultimately lead to initiation of cracking. Similar results are shown in Table 10 for suspended joints.

Table 9. Contours of Contact Pressure in Supported Joint Under 35.75-kip Wheel Load

<p>Supported Joint</p> 	<p>4 bolts Easement Configuratio n 1</p>		
	<p>4 bolts Easement Configuratio n 2</p>		
	<p>6 bolts Easement</p>		
	<p>4 bolts No Easement Configuratio n 1</p>		
	<p>4 bolts No Easement Configuratio n 2</p>		
	<p>6 bolts No Easement</p>		

Note: Contours set to indicate pressure greater than 1 psi

Table 10. Contours of Contact Pressure in Suspended Joint Under 35.75-kip Wheel Load

<p>Suspended Joint</p> 	<p>4 bolts Easement Configuration 1</p>		
	<p>4 bolts Easement Configuration 2</p>		
	<p>6 bolts Easement</p>		
	<p>4 bolts No Easement Configuration 1</p>		
	<p>4 bolts No Easement Configuration 2</p>		
	<p>6 bolts No Easement</p>		

Note: Contours set to indicate pressure greater than 1 psi.

The FEA was used to estimate the change in bolt tension before and after the application of a wheel load at the joint. Table 11 contains bar graphs which represent the tension in each bolt before and after a wheel load of 35.75 kips is applied directly over the center of a supported rail joint with different bolt configurations. Table 12 shows the corresponding results for suspended joints. Both tables include results with and without easement, which appears to have a negligible effect on the change in bolt tension.

In all suspended joint cases, bolt tension increases in every bolt when wheel load is introduced, while bolt tension decreases in every bolt when wheel load is introduced in all supported joint cases. In the suspended joints with four bolts in configuration 1, the bolts in the two innermost holes experience the greatest increase in tension under wheel loads.

Table 11. Bolt Tension in Supported Joint Before and After 35.75-kip Wheel Load

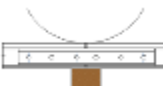
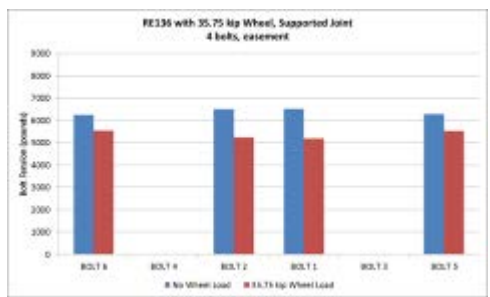
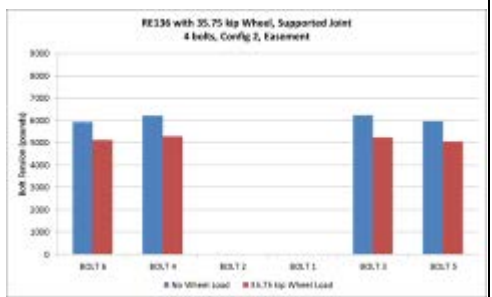
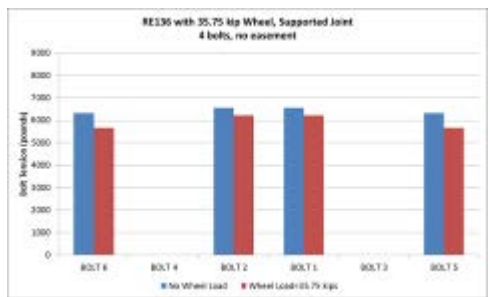
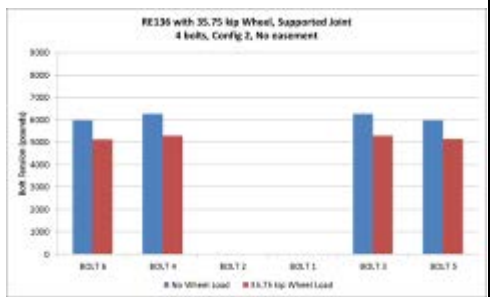
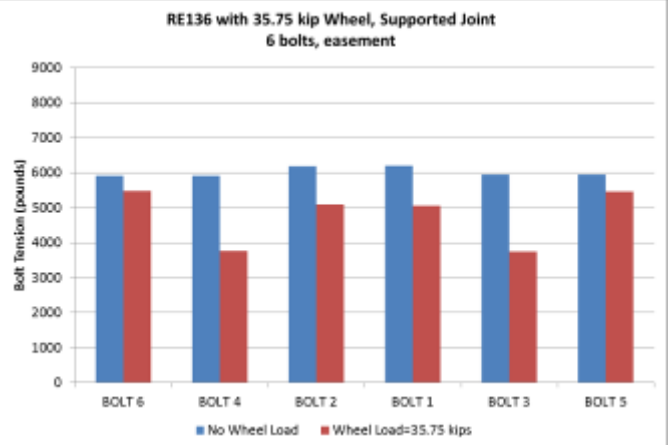
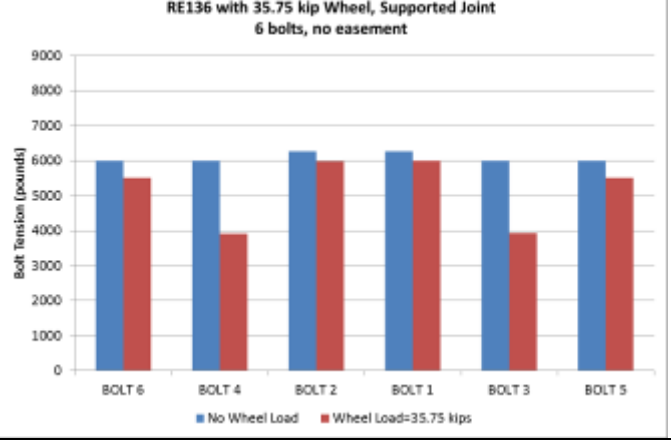
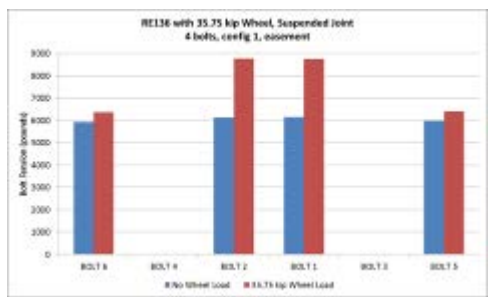
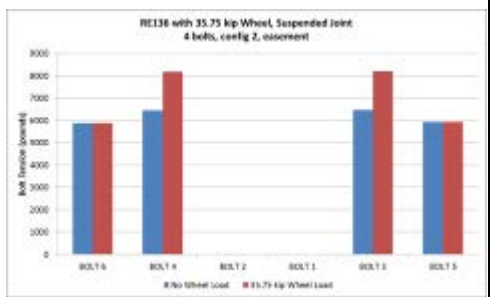
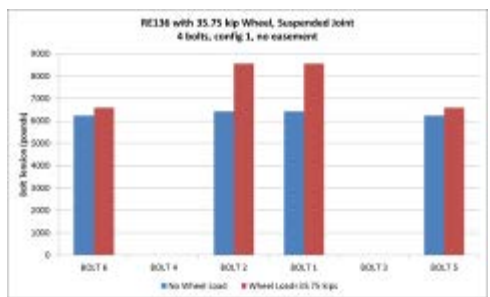
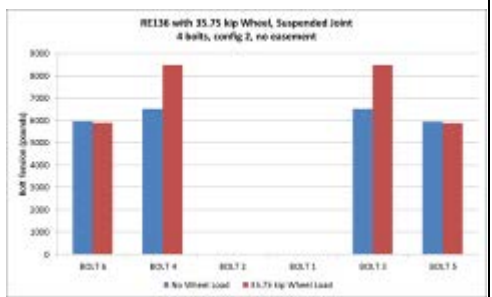
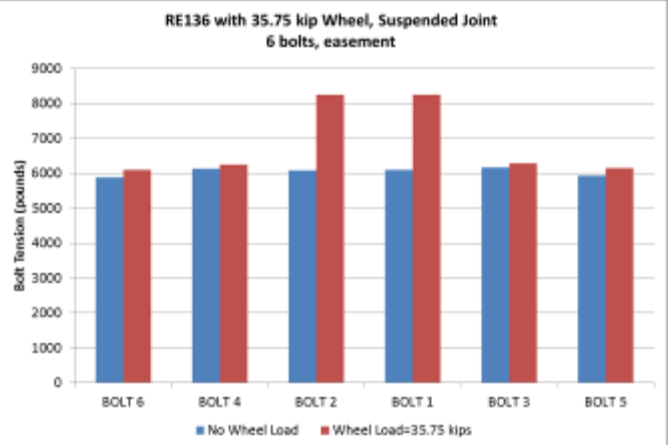
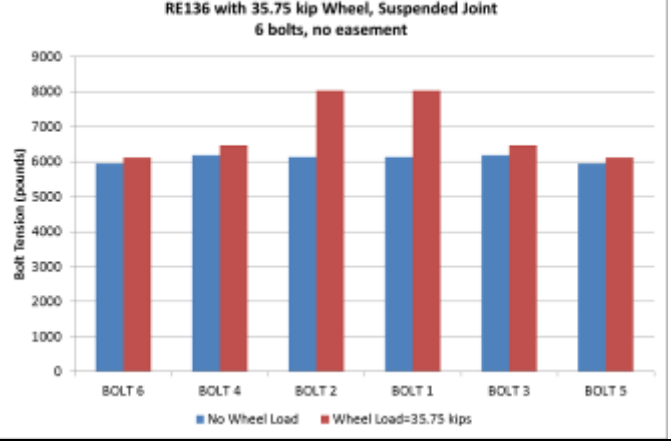
 Supported Joint	4 bolts – Easement	Configuration 1 	Configuration 2 
	4 bolts – No Easement	Configuration 1 	Configuration 2 
	6 bolts – Easement	RE136 with 35.75 kip Wheel, Supported Joint 6 bolts, easement 	
	6 bolts – No Easement	RE136 with 35.75 kip Wheel, Supported Joint 6 bolts, no easement 	

Table 12. Bolt Tension in Suspended Joint Before and After 35.75-kip Wheel Load

 <p>Suspended Joint</p>	4 bolts – Easement	Configuration 1 	Configuration 2 
	4 bolts – No Easement	Configuration 1 	Configuration 2 
	6 bolts – Easement	RE136 with 35.75 kip Wheel, Suspended Joint 6 bolts, easement 	
	6 bolts – No Easement	RE136 with 35.75 kip Wheel, Suspended Joint 6 bolts, no easement 	

8. Industry Design Developments

While joint bar design has remained relatively unchanged for many years, recent industry research and development activity in bonded insulated joints has resulted in significant improvements in performance of these components over the past 10 years. Some of those improvements can also be applied to standard (non-insulated) rail joints. Current joint bar designs originated in the period when most track was comprised of jointed rail. The bars were developed to allow relative longitudinal movement of the rails (with respect to each other) in a joint [8]. This feature is not desirable in CWR track because relative movement can be the cause of some of the failure modes described in the previous sections of this report.

Railway track standards engineers and rail joint suppliers are working on various designs that will allow less relative movement of rail joint components under load. This is expected to reduce:

- Variations in rail end gaps
- Vertical deflections under load
- Rail end gouging on joint bar top surfaces

A nonproprietary example of these designs is shown in Figure 36 [8]. The bar provides for more contact area with the rail in the web and corner fillets. Figure 37 compares the rail contact areas of the standard and new design joint bars. This larger area is intended to increase longitudinal load carry capacity before allowing rail slippage. The cross section also allows for an easement at the top of the bar. This is intended to reduce the gouging seen on the tops of some current bars from which joint bar cracking is known to occur. This design also claims to reduce bar stresses near bolt holes by improving bar support in this area.



Figure 36. Example Prototype Joint Bar Design

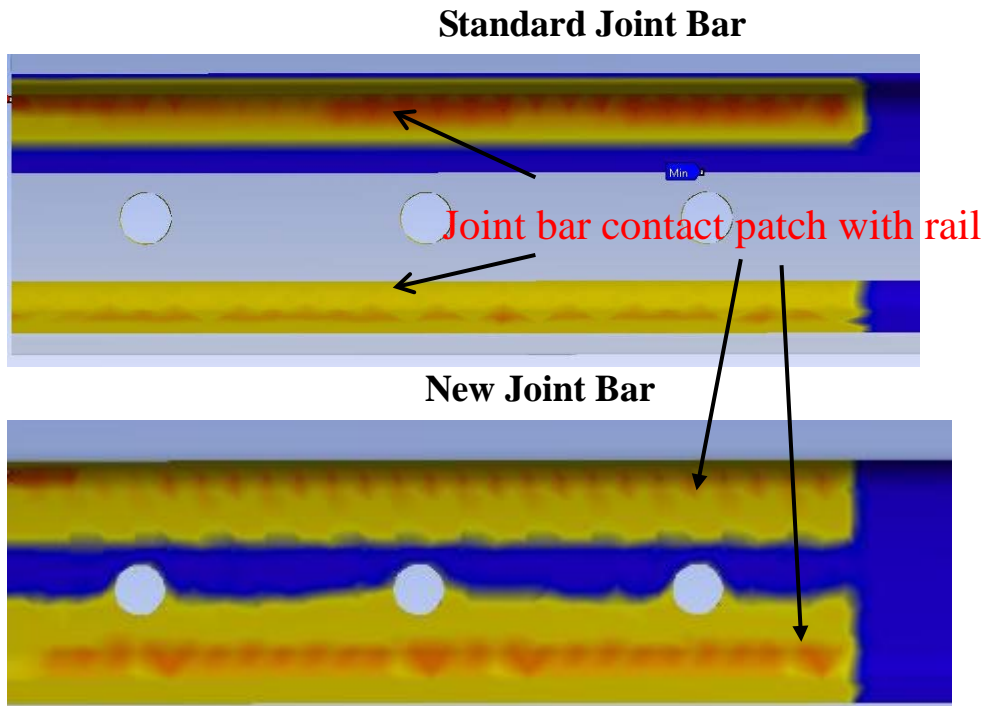


Figure 37. Calculated Contact between Rail and Joint Bar by Design

These designs are currently in the prototype development and testing phase. By addressing the current failure modes, this design offers the promise of reducing failures and may lead to improved safety and longer service lives for rail joints.

9. Conclusions

TTCI conducted several tests under the sponsorship of the FRA's Office of Research, Development, and Technology to investigate the effect of service environment on joint bar performance. Findings from the final part of this three-part series are as follows:

- Rail joint deflection under load is highly dependent on support conditions in the vicinity of the joint. Furthermore, rail joint deflections are highly correlated with failed or defective joint bars. As the previous phases of this study showed, limiting joint deflection will extend joint bar service life significantly [1,2].
- Track surfacing is probably not the cause of crack development at the top longitudinal center of the joint bars. Measured joint bar strains from surfacing, including the raising and lowering of the rail joints, were low. Tensile strains on the top of the bars were lower than typically seen from train operations (5 ksi versus 10–20 ksi). The top of the bars had largely compressive strains for most of the surfacing done to raise joints that were lower than 1 in.
- Joint bar cracking at the top longitudinal center is likely due to notching from contact with the ends of the railheads under load. Surface hardening of joint bars to improve the resistance to notching from railhead-edge contact was largely ineffective. Comparisons of hardened and unhardened joint bars under HAL operations revealed that both types of bars had metal flow at the top center of the bars. While there may be some benefit in reducing the amount of metal flow, the contact conditions are sufficiently severe to cause plastic deformation. This result suggests that a review of the joint bar easement design may be beneficial.
- The effects of rail end gaps at joints were measured under a HAL train consist. Rail joints produce some dynamic load as compared to continuous rail. However, the effect of varying the rail end gap from 0 to 1 in was small over the range of speeds tested (i.e., 10–45 mph), which may be due to the IWS' inability to capture the impact events experienced by the rail joints during testing.
- The effect of rail height mismatch at joints was measured under a HAL train consist as well. Again, the effect was relatively small in terms of joint bar strains, possibly due once more to the use of IWS for this testing. However, the measured wheel/rail forces, which were relatively low, also suggest that the test may not represent revenue service conditions.
- There was little correlation between joint bar surface hardness and metal flow depth at the top center of joint bars, which suggests that a simple measure of flow depth cannot yet be used to reject joint bars from being re-used in track. A larger sample, including more cracked bars, is needed to reach a definitive conclusion.
- Results from FEAs of bolted rail joints show that vertical deflections depend strongly on support conditions in the vicinity of the joint. These results are consistent with measurements from field surveys on joints in revenue service and with the results from tests conducted by TTCI. FEAs also show that the locations of contact and the relative magnitude of the contact pressure between the rail and the joint bar depend on the

number of bolts as well as support conditions. Furthermore, these results indicate that the contact forces at the top of the joint bar are lower when an easement is present compared to those on a bar without an easement.

10. References

1. Akhtar, M. and Davis, D. (April 2013). “Load Environment of Rail Joint Bars – Phase I, Effects of Track Parameters on Stresses and Crack Growth.” DOT/FRA/ORD-13/24, Federal Railroad Administration, Washington, DC.
2. Akhtar, M., Koch, K., Wiley, R., Davis, D. (to be published). “Load Environment of Rail Joint Bars – Phase II, Joint Bar Service Environment and Fatigue Analysis.” DOT/FRA/ORD-13/XX, Federal Railroad Administration, Washington, DC.
3. Jeong, D.Y., Bruzek, R., Tajaddini, A. (April 2014). “Engineering Studies on Joint Bar Integrity, Part I: Field Surveys and Observed Failure Modes.” JRC2014-3706. *Proceedings of the 2014 Joint Rail Conference*, Colorado Springs, CO.
4. Li, D., Meddah, A., Davis, D.D., Kohake, E. (December 2006). “Measurement of Load Environment and performance of Insulated joints at Western Mega Site.” *Technology Digest* TD-06-028, Association of American Railroads, Transportation Technology Center, Inc., Pueblo, CO.
5. Carolan, M.E., Jeong, D.Y., Perlman, A.B. (April 2014). “Engineering Studies on Joint Bar Integrity, Part II: Finite Element Analyses.” JRC2014-3708. *Proceedings of the 2014 Joint Rail Conference*, Colorado Springs, CO.
6. American Railway Engineering and Maintenance-of-Way Association. (1999). *AREMA Manual for Railway Engineering, Vol. 1, Track*, Lanham, MD.
7. Hetényi, M. *Beams on Elastic Foundation*. (1974). University of Michigan Press, Ann Arbor, MI.
8. Akhtar, M., Sammon, D., and Davis, D. (April 2013). “Improved Joint Bar Profile for Heavy Axle Load Environment.” *Technology Digest* TD-13-009, Association of American Railroads, Transportation Technology Center, Inc., Pueblo, CO.

Abbreviations and Acronyms

BHN	Brinell Hardness Number
CCW	Counterclockwise
CW	Clockwise
CWR	Continuous welded rail
FAST	Facility for Accelerated Service Testing
FEA	Finite element analysis
FRA	Federal Railroad Administration
HAL	Heavy axle load
Hz	Hertz
IWS	Instrumented wheelset
JBIS	Joint Bar Inspection System
ksi	Thousand pounds per square inch
MGT	Million gross tons
mph	Miles per hour
NDE	Nondestructive examination
psi	Pounds per square inch
RE	Railway eng
TOR	Top of rail
TTC	Transportation Technology Center (the site)
TTCI	Transportation Technology Center, Inc. (the company)
VL1	Vertical force, left wheel, axle one
VL2	Vertical force, left wheel, axle two
VR1	Vertical force, right wheel, axle one
VR2	Vertical force, right wheel, axle two